Anti-tumor effect induced by both DNA vaccine and oncolytic adenovirus expressing multi-target genes related to immunity in malignant melanoma

Soyoung Kim

Department of Medical Science

The Graduate School, Yonsei University

Anti-tumor effect induced by both DNA vaccine and oncolytic adenovirus expressing multi-target genes related to immunity in malignant melanoma

Directed by Professor Joo-Hang Kim

The Doctoral Dissertation
submitted to the Department of Medical Science,
the Graduate School of Yonsei University
in partial fulfillment of the requirements for the degree
of Doctor of Philosophy

Soyoung Kim

December 2014

This certifies that the Doctoral Dissertation of Soyoung Kim is approved.

Thesis Supervisor: Joo-Hang Kim

Thesis Committee Member #1: Jae Jin Song

Thesis Committee Member #2: Jeon Han Park

Thesis Committee Member #3: Jinsil Seong

Thesis Committee Member #4: Byoung Chul Cho

The Graduate School
Yonsei University

December 2014

<TABLE OF CONTENTS>

ABSTRACT ····· 1

I. INTRODUCTION ····· 5

II. MATERIALS AND METHODS ····· 13

1. Construction of stable cell line expressing CAR and E1B55KDa ····· 13

2. Cell culture ····· 13

3. Construction of GFP expressing replication-defective adenoviral vector ····· 14

4. Construction of oncolytic adenoviral vectors ····· 14

A. E3 region - shuttle vector cloning and homologouse recombination ····· 14

B. E1 region - shuttle vector cloning and homologouse recombination ····· 15

5. Oncolytic recombinant adenoviruses ····· 17

6. Flow cytometric analysis ····· 18

7. Cytopathic effect assay ····· 18

8. Murine spleen cell preparation ····· 19

9. Lactate dehydrogenase assay (LDH assay) ·····19
10. Western blot analysis·····20
11. Real-time polymerase chain reaction·····21
12. Enzyme-linked immunosorbent assay (ELISA) ·····22
13. Animal study ·····22
14. Immunohistochemistry (IHC)·····24
15. Preparation of B16BL6 cell lysate·····25
16. IFN-γ enzyme-linked immune spot (ELISPOT) assay·····26
17. Statistical analysis·····26
III. RESULTS·····28
1. Establishment of a cell line for adenovirus infection and replication·····28
2. Induction of an mouse melanoma antigen-specific immune response using human MART1 in mouse melanoma cells·····31
3. Downregulation of TGF-β in melanoma cells·····34
4. Construction and transfection of recombinant adenovirus expressing both mGM-CSF and shmTGF-β2·····39

5. Ex vivo and in vivo testing of combination treatment with shmTGF-β2 and mGM-CSF ····· 43
6. Construction of a recombinant adenovirus expressing MART1, mGM-CSF and shmTGF-β2 ····· 46
7. Enhanced expression of MART, mGM-CSF and downregulation of mTGF-β2 in MGT virus-infected mouse melanoma cells ····· 49
8. In vivo effects of combination treatment with recombinant MART1 plasmid with recombinant oncolytic adenovirus expressing MART1, mGM-CSF, and shmTGF-β2 ····· 53
9. Immune priming/boosting effect of repeated administration of MART1 plasmid and treatment with recombinant adenovirus expressing MART1 ····· 59
10. Enhanced anti-tumor effects and survival rate following repeated MART1 plasmid injections combined with MGT virus treatment ····· 62

IV. DISCUSSION ····· 71

V. CONCLUSION ····· 79

REFERENCES ····· 80

ABSTRACT (IN KOREAN) ·····88

PUBLICATION LIST·····92

LIST OF FIGURES

Figure 1. Schematic representation of the combination therapy developed in this study ····· 12
Figure 2. Infectivity of adenovirus in B16BL6-CAR/E1B55 cell line ····· 29
Figure 3. Mouse melanoma antigen-specific immune priming effect of human MART1 plasmid ····· 33
Figure 4. Schematic representation of shmTGF-β expressing adenovirus vectors ····· 36
Figure 5. TGF-β transcriptional level and change in cell-signaling molecules by shmTGF-β1 and shmTGF-β2 expressing adenoviruses ····· 38
Figure 6. mGM-CSF and shmTGF-β2 expressing recombinant adenoviruses ····· 41
Figure 7. The anti-tumor effect of adenovirus expressing mGM-CSF with shmTGF-β2 ····· 45
Figure 8. Schematic representation of recombinant adenovirus vectors expressing MART1/mGM-CSF/shmTGF-β2 and cytotoxic activity of viruses ····· 47
Figure 9. The expression levels of MART1, mGM-CSF and shmTGF-β2 in virus infected cells ····· 51
Figure 10. Anti-tumor effect of the combination treatment of MART1 plasmid with adenovirus expressing

MART1, mGM-CSF, and shmTGF-β2 ····· 56
Figure 11. Tumor xenografts ····· 57
Figure 12. Immunohistochemical analysis of recombinant adenovirus infected tumor sections ····· 58
Figure 13. Effect of repeated administration of the MART1 plasmid ····· 60
Figure 14. Anti-tumor effects induced by treatment with the recombinant MART1 plasmid and the recombinant oncolytic adenovirus expressing MART1, mGM-CSF and shmTGF-β2 ····· 65
Figure 15. Tumor growth and consequent survival rate of tumor-bearing mice ····· 66
Figure 16. Enhanced mouse melanoma antigen-specific anti-tumor activity of immune cells ····· 68
Figure 17. Detection of infiltrated immune cells by immunohistochemistry ····· 70

ABSTRACT

Anti-tumor effect induced by both DNA vaccine and
oncolytic adenovirus expressing multi-target genes related to immunity
in malignant melanoma

Soyoung Kim

Department of Medical Science
The Graduate School, Yonsei University

(Directed by Professor Joo-Hang Kim)

Immunogene therapy is an immune system-mediated strategy for cancer treatment that involves the delivery of immune-modulating genes to the tumor site to induce an adaptive anti-tumor immune response in the host.

This study was designed to develop a novel anti-cancer immunogene therapy effective against malignant melanoma in the C57BL/6 mouse model. A recombinant plasmid containing MART1, a human melanoma-specific tumor antigen, was used to induce an immune reaction against the mouse melan-A epitope in order to overcome the peripheral tolerance of the mouse to murine melan-A. In addition, mouse

granulocyte macrophage-colony stimulating factor (mGM-CSF) and short hairpin RNA against mouse transforming growth factor-β2 (shmTGF-β2) genes were delivered together with MART1, because GM-CSF is known to be the most potent inducer of antitumor immunity, and TGF-β is known to be involved in tumor survival and host immune suppression. These genes were delivered to cancer cells by using an oncolytic adenovirus. A recombinant DNA expressing human MART1 (MART1 plasmid) and a recombinant adenovirus expressing human MART1 were investigated for their potential effects on priming and boosting immune responses.

First, the expression of MART1 was increased in MART1 plasmid-transfected B16BL6 mouse melanoma cells in a dose-dependent manner in vitro. Notably, the cytotoxic activity of splenocytes isolated from MART1 plasmid-injected non-tumor-bearing mice was enhanced compared to those isolated from control plasmid-injected mice.

Thus, recombinant oncolytic adenovirus expressing mGM-CSF and shmTGF-β2 were also investigated for their potential to stimulate the non-specific immune response and decrease the expression of signaling molecules involved in tumor cell survival and growth, respectively. To

this end, the effect of recombinant oncolytic adenovirus expressing both mGM-CSF and shmTGF-β2 (GT virus) was compared to that of the recombinant adenovirus expressing mGM-CSF only (G virus), following intratumoral injection of the virus into melanoma-bearing C57BL/6 mice. This investigation shows that administration of the G virus leads to delayed tumor growth compared to the empty viral control, while tumor growth in mice that received the GT virus was significantly decreased ($P < 0.001$) compared to both the control- and G virus-treated mice.

Finally, an oncolytic adenovirus expressing MART1, mGM-CSF, and shmTGF-β2 (MGT virus) was constructed and administered to boost the immune response and cancer cell death. Administration of this virus induced a stronger and longer-lived immune response than that observed in the controls. Interestingly, none of the mice that received MART1 plasmid pre-treatment in addition to MGT viral injection showed any signs of tumor growth and 100% were viable 43 days after tumor cell injection.

This study investigates the anti-tumor effects of repeated MART1 plasmid vaccination and immune stimulation/tumor cell lysis with an oncolytic adenovirus expressing MART1/mGM-CSF/shmTGF-β2. The

results presented herein highlight the function of these genes during tumorigenesis as well as the possible therapeutic options of this treatment strategy. Additional work is necessary to further evaluate the clinical application of this combination therapy to treat malignant melanoma.

Key words: malignant melanoma, immune therapy, tumor antigen, DNA vaccine, oncolytic adenovirus, MART1, GM-CSF, TGF-β2

Anti-tumor effect induced by both DNA vaccine and
oncolytic adenovirus expressing multi-target genes related to immunity
in malignant melanoma

Soyoung Kim

Department of Medical Science
The Graduate School, Yonsei University

(Directed by Professor Joo-Hang Kim)

I. INTRODUCTION

Tumors, which arise from abnormal cell proliferation in a tissue, can be benign, pre-cancerous, or malignant. There are several methods for the treatment of tumors, such as surgery, chemotherapy and radiation therapy, but these therapies have limitations to treat malignant cancer; particularly for end stage cancer, metastatic cancer, and carry a high risk of relapse. In current medical practice, most cancer patients are treated with a combination of surgery, radiation, and/or chemotherapy. Although primary tumors in an early stage of malignancy can, in most cases, be efficiently treated with a combination of these standard therapies, efforts to prevent the metastatic spread of disseminated tumor cells are not often effective when treating patients in the late or end stage

of disease progression.

The incidence of malignant melanoma is rapidly increasing worldwide [1] and is the fifth highest occurring cancer in the United States and United Kingdom [2]. Although early primary melanomas can be cured surgically, once metastases develop, this type of cancer can rapidly become fatal. Furthermore, while therapeutic agents such as ipilimumab (a therapeutic agent that targets CTLA4) and vemurafenib (a therapeutic agent used against melanoma carrying a mutation in the BRAF gene), have been developed to fight malignant melanoma, these compounds have short treatment windows and low success rates [3-6]. Therefore, new treatments are required in order to provide more options and, ideally, a better outcome for patients with late stage malignant melanoma.

Recently, to overcome these limitations, new treatment modalities have been proposed, including gene therapy/immunotherapy. Cancer immunotherapy is intended to harness the reactivity of the host's immune system to combat cancer. The main strategies of cancer immunotherapy aim to exploit the therapeutic potential of tumor-specific antibodies and cellular immune effector mechanisms. To date, adenovirus and retrovirus vectors have been the most predominantly used vectors for immunogene therapy; these are utilized in 23.3% and 19.7% of all immunotherapy treatments, respectively [7]. Many features of the adenovirus make it well suited for gene delivery systems. For example, recombinant adenovirus can be grown to high titers and has a relatively high

capacity for transgene insertion, usually without the incorporation of viral DNA into the host cell genome [8,9]. Moreover, the use of an oncolytic adenovirus in immunogene therapy will not damage normal cells, but is engineered to induce tumor-specific cell lysis [8-10]. Initial attachment of the adenovirus virion particle to the cell surface occurs through binding of the fiber knob to the coxsackievirus B and adenovirus receptor (CAR) [9]. Therefore, effective therapeutic gene delivery can be induced by using the adenoviral vector construct without any further engineering. Further, this vector can be used to transport various types of genes into the cell, without discrimination.

Notably, while immunogene therapy has shown promise in treating various types of cancer, only 0.1% of these therapies utilized in preclinical studies proceed into phase IV clinical trials [7]. The success of immunogene therapies during a clinical trial is dependent on a number of factors, including whether the immune system was primed/boosted. For example, patients who have an immunological memory for the vaccine antigen would be expected to have a quick and strong immune response to the antigen [11]. In contrast, patients with no immunological memory against the vaccine antigens will likely take more time to develop an effective antigen-specific immune response. Thus, several rounds of repeated vaccinations might be required to prime antigen-specific naive T cells to produce functional effector cells [11]. It is also possible that immune priming/boosting using a tumor antigen could help to increase the immune

response of the patient during immunogene therapy.

The injection site of the antigen, either intramuscularly or intradermally, has also been shown to be important in efficiently inducing a strong, long-lived immune response [12]. While the intradermal route of administration appears to be the most efficient, there is some evidence suggesting that either route leads to antibody production and the activation of both major histocompatibility complex (MHC) class I-restricted antigen-specific cytotoxic T lymphocytes (CTL) and MHC class II-restricted CD4+ T cells secreting Th1-type cytokines [13-15]. Intramuscular delivery of plasmid DNA vaccines has also been shown to lead to the expression of the encoded protein by a variety of cell types [16,17]. Evidence suggests that professional antigen-presenting cells (APCs) may play a dominant role in the induction of immunity and that some APCs are directly transfected with plasmid DNA, causing them to rapidly migrate to the draining lymph nodes and initiate an immune response [18,19]. Dendritic cells also play a role in cross-presenting antigen produced by transfected non-immune cells (such as muscle cells) [20,21]. Both of these pathways are known to contribute to the activation of major histocompatibility complex (MHC)-matched CD8+ T cells, which then function to kill target cells and produce IFN-γ, an important activator of macrophage and inducer of class II MHC molecule expression [22]. As a result, these pathways can stimulate innate and adaptive immunity.

Furthermore, in terms of immunity induction, plasmid DNA immunization

has several potential advantages compared with traditional protein vaccination regardless of the injection site and has been shown to activate strong CTL and Th1 responses as well as resist antibody-mediated clearance, prolonging antigen expression [13-15,23-25]. Currently, the primary types of anti-cancer genes that have been delivered to tumor sites via plasmid DNA/vector injection are antigen (20.5% of all immunotherapy treatments) and cytokine (18.4%) genes [7]. While plasmid DNA vaccination with a single gene may evoke an immune response, single gene treatments targeting cancer have not shown high cure rates, likely because tumor cells have various immune evasion techniques [26]. Thus, to induce a more effective anti-tumor effect, combination treatment with multiple therapeutic genes is likely necessary. In this study, I have focused on the use of GM-CSF (a cytokine), shRNA against TGF-β (an immunomodulatory protein), and MART1 (a human melanoma antigen) to determine their effectiveness when used in combination immunogene therapy to treat malignant melanoma.

MART1 (melan-A), a human melanocyte lineage-specific protein, is expressed by 75–100% of melanomas, but is not detected in other cell or tumor types [27]. Further, Butterfield et al. previously showed that vaccination with dendritic cells transduced with human MART1 protected against the murine counterpart of this melanocyte-lineage antigen [28]. The basis of this cross-species protective response may related to the nearly 70% shared amino acid sequence [28]. Therefore, administering MART1 plasmid as well as recombinant adenovirus

vector expressing MART1 would be expected to stimulate a stronger mouse melanoma antigen-specific immune response (essentially acting to prime/boost the system).

Granulocyte macrophage-colony stimulating factor (GM-CSF), which is known to play an important role in the activation of immune cells, is expressed by a variety of cell types, including macrophage, T cells, mast cells, natural killer (NK) cells, endothelial cells, and fibroblasts [29,30]. Because GM-CSF is a major factor involved in the immune response (non-specific) and is known to effectively induce a targeted immune response to melanoma cells [31], it is a good therapeutic candidate for immunogene treatment of this specific form of cancer.

Transforming growth factor (TGF)-β is secreted in an autocrine and paracrine fashion by a variety of cell types in the tumor microenvironment, including the tumor cells, immune cells, and fibroblasts [32]. There are three isoforms of TGF-β: TGF-β1 (expressed in epithelial, endothelial, hematopoietic, and connective tissue cells); TGF-β2 (expressed in epithelial and neuronal cells); and TGF-β3 (expressed primarily in mesenchymal cells) [33-35]. TGF-β signals are known to have important roles in cell proliferation, differentiation, angiogenesis, and wound healing [36,37]. In addition, TGF-β signaling helps cancer cells repress the immune response of certain cell types, including NK cells, dendritic cells, macrophage, and T cells, while also inducing the activation of regulatory T cells [38]. Thus, reducing the expression of TGF-β in malignant melanoma would be

expected to inhibit the survival of tumor cells and induce activation of the immune system.

In oncology, an inadequate immune response towards a tumor permits tumor growth [39]. Therefore, a successful DNA vaccine for the treatment of tumors should essentially break the cancer cell's established immune tolerance to the tumor antigen, inducing a strong, prolonged tumor-specific immune response. In Chapter III: RESULTS, I have outlined my findings concerning the use of mGM-CSF, shRNA against mTGF-β, and MART1 to treat malignant melanoma. With this investigation I have demonstrated that the combination of the MART1 plasmid with an oncolytic adenovirus construct expressing MART1, mGM-CSF, and shmTGF-β2 have a pronounced anti-tumor effect on melanoma cells. (Fig 1)

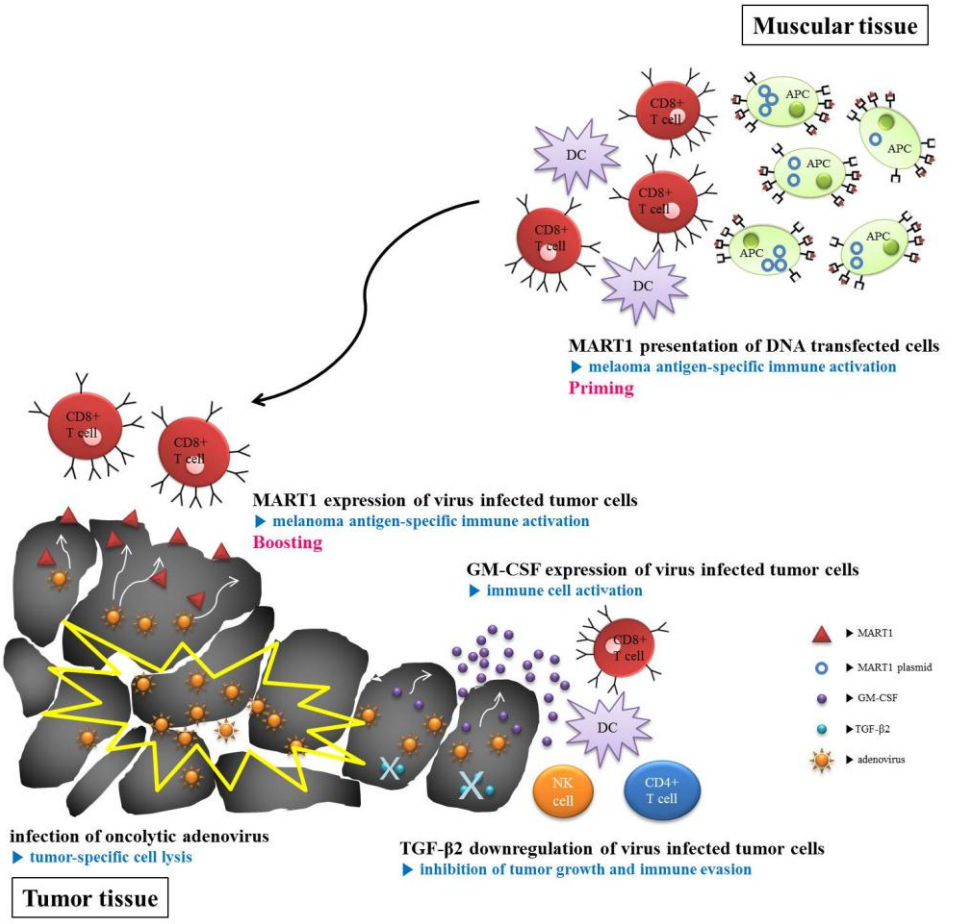

Figure 1. Schematic representation of the combination therapy developed in this study. To develop an improved cure for malignant melanoma, MART1 plasmid together with oncolytic adenovirus expressing MART1, mGM-CSF, and shmTGF-β2 were treated.

II. MATERIALS AND METHODS

1. Construction of stable cell line expressing CAR and E1B55KDa

After transfection with the pIRES-CAR/E1B55 plasmid expressing both CAR and E1B55 (one of the adenovirus proteins) proteins, B16BL6 cells were cultured in minimum essential medium (MEM, HyClone, Logan, UT, USA) with 10% fetal bovine serum (FBS), MEM vitamin solution (HyClone), and 0.5 mg/mL of G418 (Calbiochem, La Jolla, CA, USA) as selection medium. The medium was changed every 2–3 days after transfection. Positive clones expressing both CAR and E1B55KDa protein were then selected and named B16BL6-CAR/E1B55. B16BL6-CAR/E1B55 cells were cultured in MEM with 10% FBS, MEM vitamin solution, and 0.5 mg/mL of G418 and maintained in a 37℃ humidified atmosphere containing 5% CO_2.

2. Cell culture

The B16BL6 (mouse melanoma) cell line was cultured in MEM with 10% FBS and MEM vitamin solution. NIH-3T3 (mouse embryo fibroblast), B16F10 (mouse melanoma), LLC (Lewis lung carcinoma), A375 (human melanoma), and 293 (human embryonic kidney) cell lines were cultured in Dulbecco's modified Eagle's medium (DMEM, HyClone) with 10% FBS. SK-MEL-2 (human melanoma), SK-MEL-3 (human melanoma), and SK-MEL-28 (human

melanoma) were cultured in Roswell Park Memorial Institute (RPMI)-1640 (HyClone) with 10% FBS. Cells were maintained in a 37℃ humidified atmosphere containing 5% CO_2.

3. Construction of GFP expressing replication-defective adenoviral vector

The EGFP originated from pEGFP-N1 (Clontech Laboratories, Mountain View, CA, USA) and was cloned into the pCA14 vector by digestion using the restriction enzymes *Xho*I and *Xba*I. After linearization by *Xmn*I digestion, it was co-transformed into *Escherichia coli* BJ5183 with the Bsp119I-digested adenoviral vector (dl324-BstBI: adenovirus vector with an E1 and E3 region deletion) for homologous recombination.

To verify the homologous recombination, the plasmid DNA purified from the overnight *E. coli* culture was digested with *Hind*III and the digestion pattern was analyzed. The homologous recombinant adenoviral plasmid DNA was digested with *Pac*I and transfected into 293 cells to generate replication-deficient adenovirus.

4. Construction of oncolytic adenoviral vectors

A. E3 region – shuttle vector cloning and homologous recombination

For the expression of siRNA targeting mTGF-β1 or mTGF-β2, the short hairpin RNA (shRNA) construct was cloned into pSP72ΔE3-U6 vector by

digestion with *BamH*I and *Hind*III. These vectors named pSP72ΔE3-U6-shmTGF-β1 and pSP72ΔE3-U6-shmTGF-β2 (E3 shuttle vector). The U6 promoter of pSP72ΔE3-U6-shmTGFβ2 plasmid was replaced with H1 promoter through digestion with *Sph*I and *BamH*I. And then U6 promoter-shmTGFβ1-SV40 construct from pSP72ΔE3-U6-shmTGFβ1 (*Sph*I-blunt-*Kpn*I) was cloned into the pSP72ΔE3-H1-shmTGFβ2 plasmid (*Hind*III-blunt-*Kpn*I). This recombinant E3 shuttle vector was called pSP72ΔE3-H1-shmTGFβ2-U6-shmTGFβ1. These recombinant shuttle vectors were linearized by *Xmn*I digestion and co-transformed into *E. coli* BJ5183 together with the *Spe*I-digested adenoviral vector (dl324-BstBI) for homologous recombination. The E1 shuttle vector was then linearized by *Pme*I digestion and co-transformed into *E. coli* BJ5183 with the BstBI-digested dl324-BstBI-ΔE3-U6-shmTGFβ1, dl324-BstBI-ΔE3-H1-shmTGFβ2 or dl324-BstBI-ΔE3-H1-shmTGFβ2-U6-shmTGFβ1 for homologous recombination.

B. E1 region – shuttle vector cloning and homologous recombination

For the construction of oncolytic adenoviral E1 shuttle vector, inverted terminal repeats (ITR)-packaging signal-mouse survivin promoter-E1A-BGH polyA construct from pBSK[3484][40] was cloned into *Hind*Ⅲ/*Eco*RI digested pVAX1 and this vector was called pVAX1-3484-ΔE1B. And then the E1R gene

of adenovirus from pCA14 (*Stu*I-blunt-*EcoR*I) was cloned into the pVAX1-3484-ΔE1B vector (*Apa*I-blunt-*EcoR*I). This recombinant vector was named pVAX1-3484--ΔE1B-E1R. The mouse survivin promoter was replaced with CMV promoter, through digestion with *Kpn*I and *Xho*I. pcDNA3.1-Hygro^{+} was used as a template for PCR amplification of the CMV promoter, with the sense primer, 5'-CGGGGTACCGATGTACGGGCCAGAT-3', and the anti-sense primer, 5'-CCGCTCGAGAATTTCGATAAGCCAG-3'. Following digestion of the PCR product of the CMV promoter with *Kpn*I/*Xho*I, it was inserted into *Kpn*I/*Xho*I-digested pVAX1-3484-ΔE1B-E1R. This recombinant oncolytic E1 shuttle vector was called pVAX1-3484-CMV-ΔE1B.

For the expression of MART1 (pVAX1-MART1, a gift from Dr. Butterfield, University of Pittsburgh, PA, USA) and mGM-CSF (Invivogen, San Diego, CA, USA), genes were cloned into the pIRES vector using *Nhe*I/*Mlu*I and *Xba*I/*Not*I restriction sites. The [CMVp-MART1-IRES], [CMVp-IRES -mGM-CSF], and [CMVp-MART1-IRES-mGM-CSF] constructs were then cloned into BglII/SalI digested pVAX1-3484-CMV-ΔE1B vector and this plasmid was named as pVAX1-3484-CMV-ΔE1B-MART1, pVAX1-3484 -CMV-ΔE1B-mGM-CSF, and pVAX1-3484-CMV-ΔE1B-MART1-IRES-mGM-CSF. These vectors are oncolytic E1 shuttle vectors. The E1 shuttle vector was then linearized by *Pme*I digestion and co-transformed into *E. coli* BJ5183 with the BstBI-digested dl324-BstBI or dl324-BstBI-ΔE3-H1

-shmTGF-β2 for homologous recombination.

5. Oncolytic recombinant adenoviruses

C virus:

Ad3484-CMVp-ΔE1B, control virus

T1 virus:

Ad3484-CMVp-ΔE1B-ΔE3-U6-shmTGF-β1,

virus expressing a shRNA against mTGF-β1

T2 virus:

Ad3484-CMVp-ΔE1B-ΔE3-H1-shmTGF-β2,

virus expressing a shRNA against mTGF-β2

G virus:

Ad3484-CMVp-ΔE1B-CMVp-mGM-CSF,

virus expressing mGM-CSF

GT virus:

Ad3484-CMVp-ΔE1B-CMVp-mGM-CSF-ΔE3-H1-shmTGF-β2,

virus expressing mGM-CSF and a shRNA against mTGF-β2

M virus:

Ad3484-CMVp-ΔE1B-CMVp-MART1,

Virus expressing human MART1

MGT virus:

Ad3484-CMVp-ΔE1B-CMVp-MART1-IRES-mGM-CSF-ΔE3-H1-shmTGF-β2 virus expressing human MART1, mGM-CSF, and a shRNA against mTGF-β2

6. Flow cytometric analysis

After B16BL6-CAR/E1B55 cells were infected with recombinant adenovirus for two days, infected cells were trypsinized and washed twice with ice-cold phosphate buffer saline (PBS). Cells were then incubated with an anti-MART1 antibody (Santa Cruz Biotechnology, Santa Cruz, CA, USA) for 1 h at 4℃. After two washes with ice-cold PBS, cells were incubated with an APC-conjugated anti-mouse IgG (BD Biosciences, Lincoln Park, NJ, USA) antibody in the dark for 45 min at 4℃ and then washed twice with ice-cold PBS. A mouse IgG fluorescence control (BD Biosciences) antibody was used as a negative control. Finally, cells were resuspended in PBS and analyzed using a FACS Calibur flow cytometer (BD Biosciences).

7. Cytopathic effect assay

To evaluate the cytopathic effect (CPE) of several tumor-selective replication-competent adenoviruses, cells were first plated at about 80% confluence into the well of a 48-well plate. They were infected with various multiplicities of infection (MOIs) of replication-competent adenovirus. After 24 h of infection, cells were monitored daily by microscopy. When cells exhibited

lysis at the lowest MOI, the remaining cells on the plate were fixed with 4% paraformaldehyde and stained with 0.05% crystal violet.

8. Murine spleen cell preparation

The spleen was extracted from C57BL/6 mice one week after last injection of pVAX1-MART1 (a plasmid expressing MART1) or pVAX1 (control plasmid) DNA or 6 days after last injection of adenovirus. After extraction, the spleen and 1 mL of PBS were directly placed into the cell strainer in the petri dish, the spleen was mashed by using the black rubber of a syringe and splenocytes were released into the petri dish. The homogenized cell suspension was then washed twice with PBS. The splenocytes were resuspended in 4 mL of PBS per spleen and the appropriate amount of ammonium chloride lysing reagent (BD Biosciences) was added. The cells were incubated for 15 min in the dark at room temperature. Cells were washed twice with PBS and resuspended in the desired medium (RPMI-1640).

9. Lactate dehydrogenase assay (LDH assay)

The cytotoxic activity of splenocytes against tumor cells was assessed by LDH assay using the Non-radioactive cytotoxicity assay kit (Promega Corporation, Madison, WI, USA). Cancer cells were incubated for 12 h in 48-well plate at 37℃ under a humidified atmosphere of 5% CO_2 in air and then

co-cultured with splenocytes isolated from C57BL/6 mice for 4 h. For the LDH positive control, 45 μL of lysis solution (10×) was added to all wells to lyse the cells and the cells were incubated for 45 min. After 45 min of incubation, the plate was centrifuged at 250 × g for 4 min. Fifty microliters of supernatant from all wells were transferred to a fresh 96-well flat-bottom plate. Fifty microliters of reconstituted substrate mix were added to each well and the plate was then incubated for 30 min at room temperature in the dark. After 30 min, 50 μL of stop solution was added to each well and the absorbance was recorded at 490 nm within 1 h using a microplate reader (Molecular Devices Corporation, Sunnyvale, CA, USA). The percentage of splenocyte cytotoxicity was calculated using the following formula:

% Cytotoxicity = {(experimental value - effector control value - negative control value) / (positive control value - negative control value)}*100.

10. Western blot analysis

Two days after transfection with the MART1 plasmid or infection with a recombinant adenovirus, B16BL6-CAR/E1B55 cells were lysed with 1× Laemmli lysis buffer (62.5 mM Tris, pH 6.8, 2% sodium dodecyl sulfate, 10% glycerol, 0.002% bromophenol blue) and the protein concentration was determined by using the BCA Protein Assay Kit (Thermo Scientific, Fremont, CA, USA). Protein samples were then separated by sodium dodecyl sulfate-polyacrylamide gel

electrophoresis and the gels were electrotransferred onto a polyvinylidene difluoride membrane (Millipore, Billerica, MA, USA). Immunodetection was performed with anti-Src (Cell Signaling Technology, Beverly, MA, USA), anti-phospho Src (pSrc) (Cell Signaling), anti-STAT3 (Cell Signaling), anti-phospho STAT3 (pSTAT3) (Cell Signaling), anti-p65 (Cell Signaling), anti-phospho p65 (pp65) (Cell Signaling), anti-β-catenin (Cell Signaling), anti-N-cadherin (Cell Signaling), anti-actin (Santa Cruz Biotechnology), anti-melanA (Santa Cruz Biotechnology), and anti-MART1 (Santa Cruz Biotechnology) antibodies by using a chemiluminescent and fluorescent image analysis system (Syngene, Cambridge, UK).

11. Real-time polymerase chain reaction

After 2 days of infection with the recombinant adenovirus, B16BL6-CAR/E1B55 cells were lysed with TRIzol reagent (Life Technologies, Carlsbad, CA, USA) and the total RNA was isolated by using chloroform. The RNA concentration was determined by using the Nanodrop 2000 (Thermo Scientific). RT-PCR was performed using the Power SYBR Green RNA-to-CT 1-Step Kit (Life Technologies). The reaction mixture contained the reverse transcriptase enzyme mix, reverse transcription PCR mix, forward primer, reverse primer, RNA template, and nuclease-free water. Mouse TGF-β1 cDNA was amplified using the forward primer: 5′-TTGCTTCAGCTCCACAGAGA-3′ and

the reverse primer: 5′-TGGTTGTAGAGGGCAAGGAC-3′. Mouse TGF-β2 cDNA was amplified using the forward primer: 5′-GTGAATGGCTCTCCTTC GAC-3′ and the reverse primer: 5′-CCTCGAGCTCTTCGCTTTTA-3′. Mouse TGF-β3 cDNA was amplified using the forward primer: 5′-CTATCAGGTCCT GGCACTTT-3′ and the reverse primer: 5′-GGCAGATTCTTGCCACCTAT-3′. Mouse β-actin was amplified using the forward primer: 5′-GGCTGTATTCCC CTCCATCG-3′ and the reverse primer: 5′-CCAGTTGGTAACAATGCCATG T-3′.

12. Enzyme-linked immunosorbent assay (ELISA)

B16BL6-CAR/E1B55 cells were plated onto six-well plates at 2×10^5 cells/well and then infected with adenoviruses (C virus, G virus, T virus, GT virus, or MGT virus) at an MOI of 50. Forty-eight hours after infection, the supernatants were harvested. mGM-CSF and mTGF-β2 level of expression was determined by using ELISAs according to the manufacturer's instructions (mGM-CSF ELISA kit and mTGF-β2 ELISA kit: R&D systems, Minneapolis, MN).

13. Animal study

Tumors were implanted subcutaneously in the abdomen of C57BL/6 mice by

injecting B16BL6-CAR/E1B55 murine melanoma cells (7×10^5) in 100 μL of Hank's balanced salt solution (HBSS; Gibco BRL, Carlsbad, CA, USA).

In the first experiment, when tumors reached a range of 70–100 mm^3, animals were randomized into 4 groups of 5 animals (PBS, Ad3484-CMVp-ΔE1B, Ad3484-CMVp-ΔE1B-CMVp-mGM-CSF, and Ad3484 -CMVp-ΔE1B-CMVp-mGM-CSF-ΔE3-H1-shmTGF-β2). Adenoviruses or PBS were administered intratumorally (virus; 1×10^9 PFU (PFU; plaque-forming unit) per tumor in 50μL of PBS) on day 1, 3, and 5.

In the second experiment, 4 days after tumor implantation, C57BL/6 mice were injected intramuscularly in the rear quadriceps with 50 μg of pVAX1-MART1 (M) encoding human MART1 in a total volume of 50 μL saline using a 29-gauge needle. When tumors reached a range of 70–100 mm^3, animals were randomized into 4 groups of 5 animals (M+PBS, M+Ad3484-CMVp-ΔE1B, M+Ad3484-CMVp-ΔE1B-CMVp-MART1, and M+ Ad3484-CMVp-ΔE1B-CMVp-MART1-IRES-mGM-CSF-ΔE3-H1-shmTGF-β2) and treatment was initiated. The first day of treatment was designated as day 1. Adenoviruses or PBS were administered intratumorally (1×10^9 PFU per tumor in 50 μL of PBS) on days 1, 3, and 5.

In the third experiment, C57BL/6 mice were injected intramuscularly in the rear quadriceps with 50 μg of pVAX1-MART1 in a total volume of 50 μL saline using a 29-gauge needle. The plasmid was injected 3 and 7 days prior to

tumor injection and 1 day after tumor injection. On day -7, tumors were implanted subcutaneously as described above. When tumors reached a range of 70–100 mm^3, animals were randomized into 4 groups of 5 animals (M+PBS, M+Ad3484-CMVp-ΔE1B, M+Ad-3484-CMVp-ΔE1B-CMVp-MART1, and M +Ad-3484-CMVp-ΔE1B-CMVp-MART1-IRES-mGM-CSF-ΔE3-H1-shmTGF-β2) and treatment was initiated. The first day of treatment was designated as day 1. Adenoviruses or PBS were administered intratumorally (1×10^9 PFU per tumor in 50 μL of PBS) on days 1, 3, and 5.

Regression of tumor growth was assessed by taking measurements of the length (L) and width (W) of the tumor. Tumor volume was calculated using the following formula: volume = $0.52 * L * W^2$.

14. Immunohistochemistry (IHC)

Immunohistochemistry studies were performed on paraffin-embedded tumor tissues using anti-CD4 (Novus Biologicals, Littleton, CO, USA), anti-NK1.1 (Novus Biologicals), anti-CD8 (Santa Cruz Biotechnology), anti-CD11b+c (Thermo Scientific), and anti-adenovirus type 5 (Novus Biologicals) antibodies to determine the expression of these proteins in the tumor tissue. The tumor tissue slides were deparaffinized by incubation in xylene for 10 min and rehydrated serially in alcohol (100%, 90%, and 70%). Endogenous peroxidase was blocked by incubation with 3% H_2O_2 for 15 min at room temperature and antigen retrieval was

achieved by incubating the slides in citrate buffer for 10 min in a steamer. For permeabilization, the slides were incubated in PBS containing 0.5% Triton X-100 for 30 min and then washed three times with PBS. To reduce nonspecific background staining due to endogenous peroxidases, the slides were incubated with a hydrogen peroxide block (Thermo Scientific) for 10 min. After washing, an ultra V block (Thermo Scientific) was applied to the slides for 5 min at room temperature to further block nonspecific background staining. The slides were incubated with an anti-CD4 antibody (1:200 dilution), an anti-CD8 antibody (1:500), anti-NK1.1 antibody (1:500), anti-CD11b+c antibody (1:500), and an anti-Ad5 antibody (1:800 dilution) for 12 h at 4℃ and further with a horseradish peroxidase polymer (Thermo Scientific) for 15 min at room temperature. To detect protein expression, the tissue sections were stained with diaminobenzidine tetrahydrochloride and minimally counterstained with hematoxylin (for visualization of antigen-antibody complexes). Sections were mounted under a coverslip using an mounting solution (Shandon Synthetic Mountant (Thermo Scientific) + xylene = 1:1).

15. Preparation of B16BL6 cell lysate

After removing the culture medium, B16BL6 cells were washed with PBS twice. Cells were then detached with a rubber policeman in 1 mL of cold PBS and transferred into a 1.5 ml tube. After centrifugation at 3000 rpm for 15 min, the

supernatant was removed. The cell pellet was resuspended with 1 mL of cold radioimmunoprecipitation assay buffer (RIPA) buffer (Thermo Scientific) with protease inhibitor (Sigma-Aldrich, St. Louis, MO, USA), and incubated on ice for 30 min with vortexing every 10 min. After centrifugation at 14000 × g for 15 min at 4℃, the supernatant, which contains the total protein, was transferred in a new tube and stored at −80℃.

16. IFN-γ enzyme-linked immune spot (ELISPOT) assay

To assess the population of antigen-specific cytokine-producing cells, IFN-γ ELISPOT assay was performed. Six days after the last adenovirus injection, the spleens were collected aseptically from mice bearing a B16BL6 tumor and unicellular splenocytes were prepared as described above. Prepared spleen cells were stimulated with B16BL6 cell lysate for 24 h in the culture medium. IFN-γ ELISPOT assay was then carried out according to the manufacturer's specifications (IFN-γ ELISPOT kit: R&D Systems). The colored spots, representing IFN-γ-producing cells, were counted with a KS-ELISpot (Zeiss-Kontron, Jena, Germany) and confirmed by the computer-based Immunospot system (AID Elispot Reader System, Version 3.4; Autoimmun Diagnostika GmbH, Strassberg, Germany).

17. Statistical analysis

Data were expressed as mean ± standard error (SE). Statistical comparison was made using SigmaPlot 8.0 (Systat Software Inc, San Jose, CA, USA). P values less than 0.05 were considered statistically significant (*, $P < 0.05$; **, $P < 0.01$;***, $P < 0.001$).

III. RESULTS

1. Establishment of a cell line for adenovirus infection and replication

Most murine cancer cell lines have a lower adenovirus infection efficiency compared to human cancer cells, as mouse cells do not express CAR. In addition, the replication rate of adenovirus is very low and this limits the effectiveness of the oncolytic adenovirus in killing mouse cancer cells. To overcome these limitations, the B16BL6-CAR/E1B55 mouse melanoma cell line was developed, which expresses both the CAR and adenoviral E1B55 genes. Notably, this transgenic cell line showed enhanced infectivity by adenovirus (Fig 2A). The replication-dependent cytotoxic effect of adenovirus in the B16BL6-CAR/E1B55 cells was also quantitatively assessed using an in vitro CPE assay. This analysis indicates that replication of the oncolytic adenovirus was induced in the B16BL6-CAR/E1B55 cells in a multiplicity of infection (MOI) value-dependent manner (Fig 2B, C).

(A)

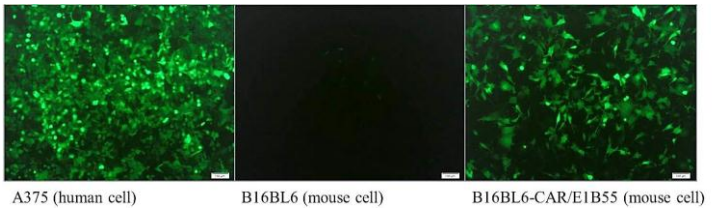

(B) (C)

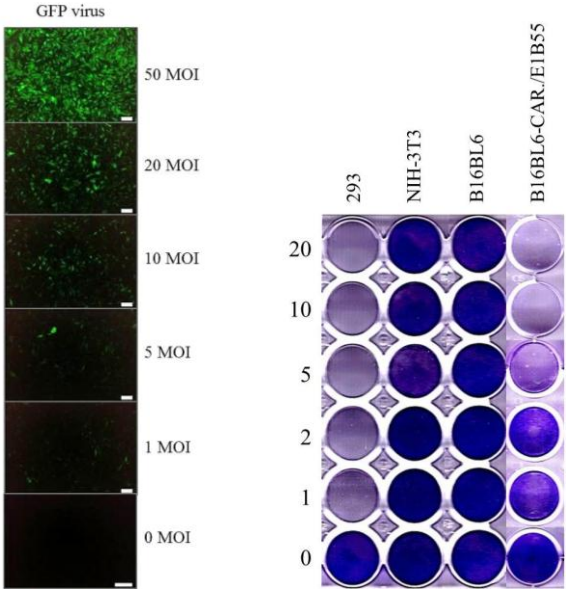

Figure 2. Infectivity of adenovirus in B16BL6-CAR/E1B55 cell line. (A) A375 (human melanoma cell line), B16BL6 (mouse melanoma cell line), and B16BL6-CAR/E1B55 were infected with adenovirus-GFP at a multiplicity of infection (MOI) of 50. After 48 h, GFP expression was detected by fluorescence microscopy (fluorescence microscope; Olympus). (B) The

B16BL6-CAR/E1B55 cell line was infected with the adenovirus at various MOIs. (C) To compare the oncolytic activity induced by Ad3484-CMVp-ΔE1B, cancer and NIH-3T3 cells were infected with virus at an MOI of 1 to 20. When 293 cells infected with the viruse at an MOI of 1 exhibited complete cell lysis, all the remaining cells on the plate were fixed with 4% paraformaldehyde and stained with 0.5% crystal violet.

2. Induction of an mouse melanoma antigen-specific immune response using human MART1 in mouse melanoma cells

Butterfield et al. (1998) previously showed that dendritic cells that were genetically modified to express the human MART1 antigen generated a potent melan-A-specific immune response in BL6 melanoma model [28]. These results imply that stimulation of MART1 could potentially induce a melan-A-specific immune response in our mouse melanoma model.

Human melanoma cell lines (including SK-MEL-2, SK-MEL-3, and SK-MEL-28) express MART1, and the murine melan-A, which shares 68.8% sequence similarity with the human form, is expressed in the mouse melanoma cell lines B16BL6 and B16F10, but not in NIH-3T3 cells (Fig 3A). Accordingly, I chose to use MART1 as a target for immune priming/boosting immunotherapy for the treatment of malignant melanoma. Further, a recombinant pVAX1-MART1 plasmid was used to express the protein, and empty pVAX1 was used as a control plasmid. Following transfection into murine melanoma cells, the expression of MART1 was observed to increase in the MART1 plasmid-transfected cells in a dose-dependent manner (Fig 3B).

To induce immune activation, 50 μg of MART1 plasmid in a total volume of 50 μl saline was injected intramuscularly into the rear quadriceps of C57BL/6 mice. This injection site was chosen because muscle cells injected with plasmid DNA have been shown to produce large amounts of the encoded protein [16,17].

Notably, injections of MART1 plasmid were administered three times, separated by a one-week interval between injections. One week after the final injection, mice were killed and their spleens were removed. To determine the effect of MART1 immune priming, splenocytes were isolated, co-cultured with B16BL6 melanoma cells, and the spontaneous release of LDH was measured. Figure 3C shows the cytotoxic activity of the splenocytes isolated from the MART1 plasmid-injected mice, which was effectively enhanced compared to that of the splenocytes isolated from the control plasmid-injected mice. This enhanced cytotoxic activity of the splenocytes also appeared to be dependent on the ratio of effector cells (splenocytes) and the target cells (B16BL6 cells). Further, activation of the immune system induced by MART1 plasmid treatment was not observed in the LLC cell line, a mouse lung cancer cell line that does not express melan-A. These data indicate that the injection of human MART1 plasmid can prime mouse melan-A-specific immunity by inducing the development of an immune cell population that is cross-reactive to both human MART1 and mouse melan-A. Based on these findings, I conclude that an effective and specific anti-tumor immune response could be induced in the B16BL6 mouse melanoma model by administering MART1 plasmid.

(A)

(B)

(C)

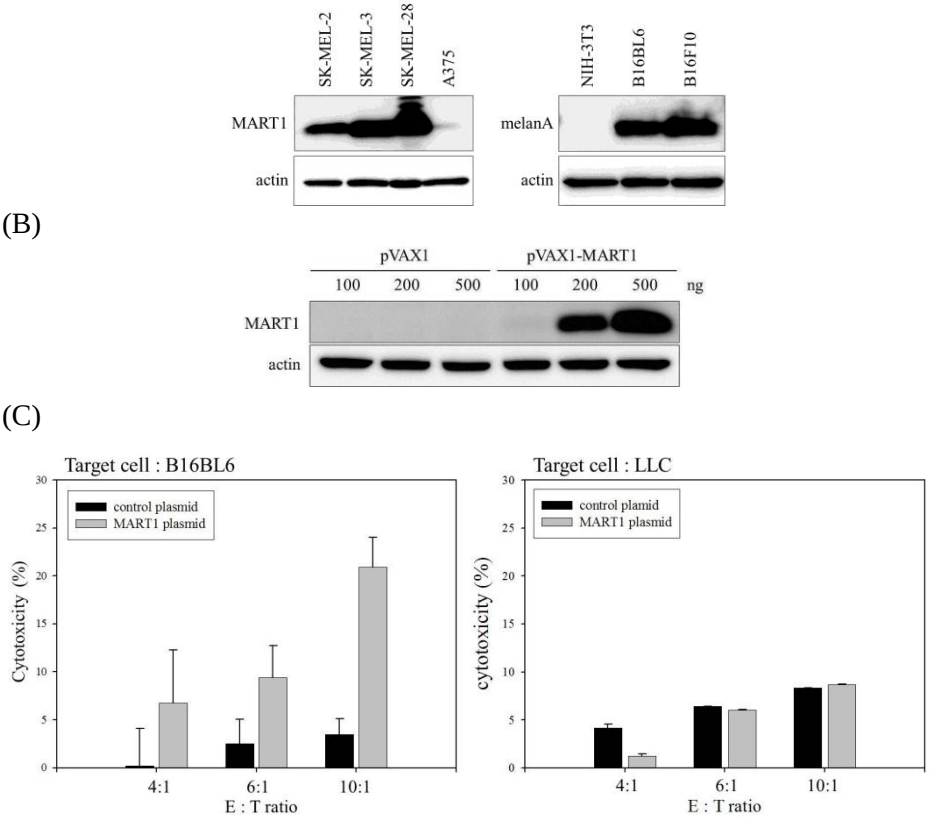

Figure 3. Mouse melanoma antigen-specific immune priming effect of human MART1 plasmid. (A) MART1 and MelanA expression were detected in various human and mouse cells by western blot. Actin was used as a loading control. (B) MART1 expression level was assessed in B16BL6 cells after transfection with pVAX1 or pVAX-MART1. (C) Splenocytes isolated from mice injected with control plasmid or MART1 plasmid were co-cultured with B16BL6 or LLC cells for 4 h. The cytotoxicity of splenocytes was then determined by LDH assay.

3. Downregulation of TGF-β in melanoma cells

Almost all human tumors overexpress TGF-β, which contributes to the induction of tumor cell invasion and metastasis [41]. Another major role of TGF-β produced by tumors is to block the immune response [42]. This local TGF-β-induced immunosuppressive environment has been shown to be the major obstacle to immunogene therapy using cytokines [43]. Accordingly, in this study shRNA against TGF-β was used as a therapeutic agent.

It has been known that TGF-β1 and TGF-β2 are highly expressed in melanoma, whereas TGF-β3 is rarely expressed. To decrease the expression of TGF-β1 and TGF-β2 protein, recombinant adenoviruses were constructed containing the shRNAs TGF-β1-sh10 and TGF-β2-sh3 (Fig 4A) individually or together (Fig 4B). Two different promoters (U6 promoter and H1 promoter) were used to prevent the formation of secondary DNA structure.

The downregulation of the mTGF-β transcripts following B16BL6-CAR/E1B55 cell infection with adenovirus expressing shRNA against mTGF-β1, mTGF-β2, or both was confirmed by real time PCR. As shown in Figure 5A, the infecting the cells with the shmTGF-β1 virus decreased the expression of mTGF-β1 mRNA level but not mTGF-β2. Similarly, treatment with shmTGF-β2 virus decreased the mTGF-β2 mRNA level by more than 50% compared to the controls. Furthermore, the endogenous cellular level of TGF-β mRNA was significantly decreased when the cells were infected with

adenovirus expressing shRNAs targeting both TGF-β1 and TGF-β2.

And then the expression levels of various endogenous signaling molecules were decreased by treatment with the shmTGF-β adenovirus. Figure 5B shows that the down-regulation of TGF-β isotypes induced changes in the expression of signaling molecules involved in cell growth, survival, or metastasis.

The expression of signaling molecules were decreased in shmTGF-β2-expressing adenovirus infected cells. But when both the TGF-β1 and TGF-β2 transcripts were silenced by infection with virus comprising both of the shmTGF-β1 and shmTGF-β2 DNA sequences, the effects on the expression of signaling molecules were lessened compared with those observed following transduction with the virus containing the shmTGF-β2 DNA sequence only. These results suggest that the downregulation of TGF-β2 is the primary TGF-β signaling molecule necessary to inhibit the growth and survival of mouse melanoma tumors. We, therefore, chose to focus on using the shmTGF-β2 construct for further investigations.

(A)

shRNA	Primer	Ct	ΔCt	ΔΔCt	$2^{-\Delta\Delta Ct}$	Reduction %
control - Trp53	actin	16.58				
	Trp53	26.50	9.92	2.30	0.20	79.69
	TGF-beta1	27.05	10.47			
TGF-beta1-sh6	actin	16.79				
	TGF-beta1	27.85	11.06	0.59	0.66	33.57
TGF-beta1-sh7	actin	16.72				
	TGF-beta1	28.60	11.88	1.41	0.38	62.37
TGF-beta1-sh8	actin	16.57				
	TGF-beta1	28.33	11.76	1.29	0.41	59.10
TGF-beta1-sh9	actin	16.55				
	TGF-beta1	28.45	11.90	1.43	0.37	62.89
TGF-beta1-sh10	actin	16.41				
	TGF-beta1	28.97	12.56	2.09	0.23	76.51
TGF-beta1-sh11	actin	16.99				
	TGF-beta1	27.89	10.90	0.43	0.74	25.77

shRNA	Primer	Ct	ΔCt	ΔΔCt	$2^{-\Delta\Delta Ct}$	Reduction %
scrambled shRNA	actin	15.84				
	Trp53	25.45	9.62			
	TGF-beta2	24.32	8.49			
control - Trp53	actin	15.61				
	Trp53	27.60	11.99	2.37	0.19	80.66
TGF-beta2-sh1	actin	16.39				
	TGF-beta2	25.28	8.89	0.40	0.76	24.21
TGF-beta2-sh2	actin	16.56				
	TGF-beta2	25.68	9.12	0.63	0.65	35.38
TGF-beta2-sh3	actin	16.08				
	TGF-beta2	26.50	10.42	1.93	0.26	73.76
TGF-beta2-sh4	actin	16.17				
	TGF-beta2	25.81	9.64	1.15	0.45	54.94
TGF-beta2-sh5	actin	16.19				
	TGF-beta2	26.25	10.06	1.57	0.34	66.32

(B)

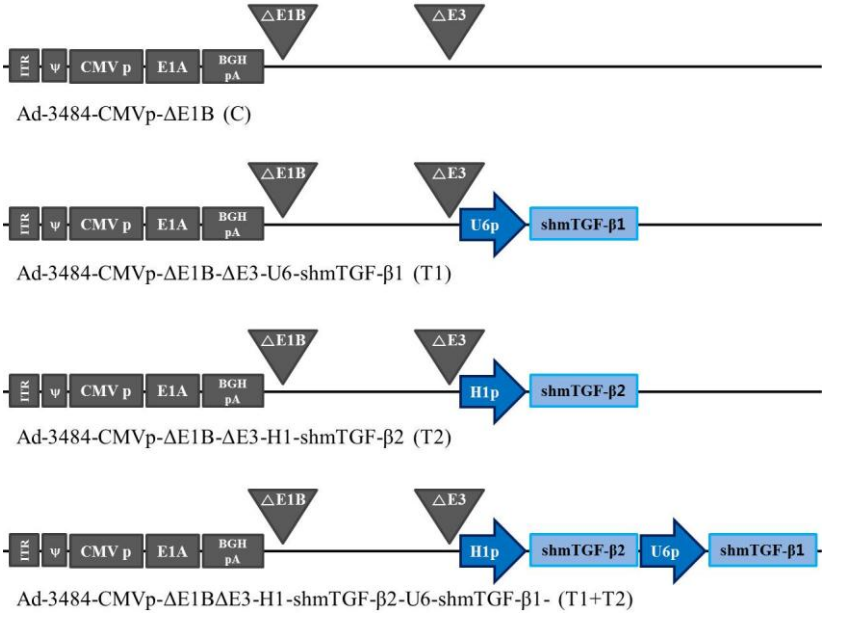

Figure 4. Schematic representation of shmTGF-β expressing adenovirus vectors. After selection of TGF-β1-sh10 and TGF-β2-sh3 to induce the down-regulation of mTGF-β1 and mTGF-β2 mRNA level (A), oncolytic adenoviruses were developed (B). Ad3484-CMVp-ΔE1B is a replication-competent adenovirus used as a control virus and contains the E1A gene controlled by the CMV promoter, but lacks the E1B gene. Ad3484-CMVp-ΔE1B-ΔE3-U6-shmTGF-β1 (T1) and Ad3484-CMVp-ΔE1B-ΔE3-H1-shmTGF-β2 (T2) are composed of the shmTGF-β1 or shmTGF-β2 genes in the E3 region of Ad3484-CMVp-ΔE1B, respectively. Ad3484-CMVp-ΔE1B-ΔE3-H1-shmTGF-β2-U6-shmTGF-β1 (T1 + T2) is composed of the shmTGF-β1 and shmTGF-β2 genes in the E3 region of Ad3484-CMVp-ΔE1B.

(A)

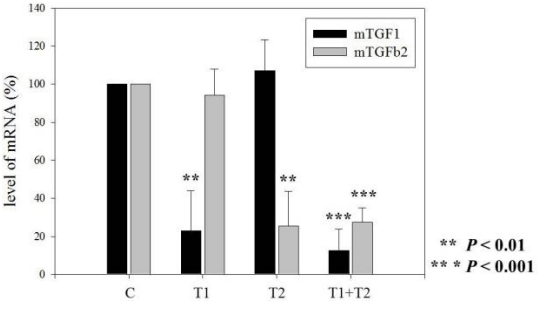

(B)

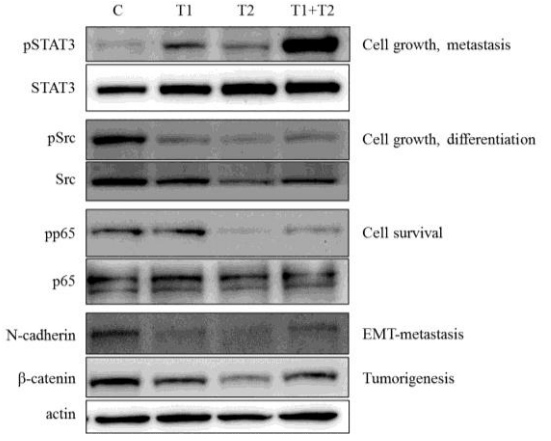

Figure 5. TGF-β transcriptional level and change in cell-signaling molecules by shmTGF-β1 and shmTGF-β2 expressing adenoviruses. (A) Relative expression level of mTGF-β1 and mTGF-β2 mRNA. C, T1, T2, or T1+T2 virus was infected into B16BL6-CAR/E1B55 cells at an MOI of 100. The knockdown efficiency of these viruses was measured by quantitative real-time polymerase chain reaction amplifying mTGF-β1 and mTGF-β2. (B) B16BL6-CAR/E1B55 cells were infected with C, T1, T2, or T1+T2 virus of 100 MOI. After two days, the endogenous expression levels of signaling molecules were detected by western blot assay. Actin was used as a loading control.

4. Construction and transfection of recombinant adenovirus expressing both mGM-CSF and shmTGF-β2

GM-CSF is a potent inducer of anti-tumor immunity that has been used as a part of various strategies to induce anti-tumor effects via tumor-reactive cytotoxic CD8+ T-lymphocytes, NK cells, and dendritic cells [44-46]. However, the systemic use of recombinant GM-CSF is compromised by side effects and the induction of potentially harmful myeloid-derived suppressor cells. Additionally, the efficacy of systemic recombinant GM-CSF treatment may remain limited as only a low local concentration of GM-CSF is found in tumors [47]. Therefore, local GM-CSF production by cancer cells could ensure a sufficient local concentration while minimizing systemic exposure. Thus, adenovirus transport and infection is an appealing molecule/technique for local delivery of GM-CSF to tumors, and the effects of this gene could possibly be further compounded by utilizing oncolytic adenoviruses.

Utilizing the results from my previous investigation concerning the role of mTGF-β2, I chose to examine the effects of combination treatment with mGM-CSF and shmTGF-β2. To develop the mGM-CSF-expressing recombinant oncolytic adenovirus, the mGM-CSF gene was inserted into the E1 region of the virus and the resulting construct was named Ad3484-CMVp-ΔE1B-CMVp-mGM-CSF (G virus). The oncolytic adenovirus expressing both mGM-CSF and shmTGF-β2 as well was named

Ad3484-CMVp-ΔE1B-CMVp-mGM-CSF-ΔE3-H1-shmTGF-β2 (GT virus) (Fig 6A). To examine the protein expression level of mGM-CSF and the mRNA expression of mTGF-β2, B16BL6-CAR/E1B55 cells were infected with virus at an MOI of 50. Two days after infection, I observed a significant increase in mGM-CSF protein (Fig 6B) and a significant reduction of mTGF-β2 mRNA (Fig 6C). The oncolytic ability of these replication-competent adenoviruses was also analyzed using an in vitro CPE assay of various cell lines (293, B16BL6-CAR/E1B55, NIH-3T3) after cells were infected with control (C), G, or GT virus at different MOIs. As shown in Figure 6D, all replication-competent adenoviruses induced an increase in CPE as the MOI increased in the B16BL6-CAR/E1B55 melanoma cancer cell line, but not in NIH-3T3.

(A)

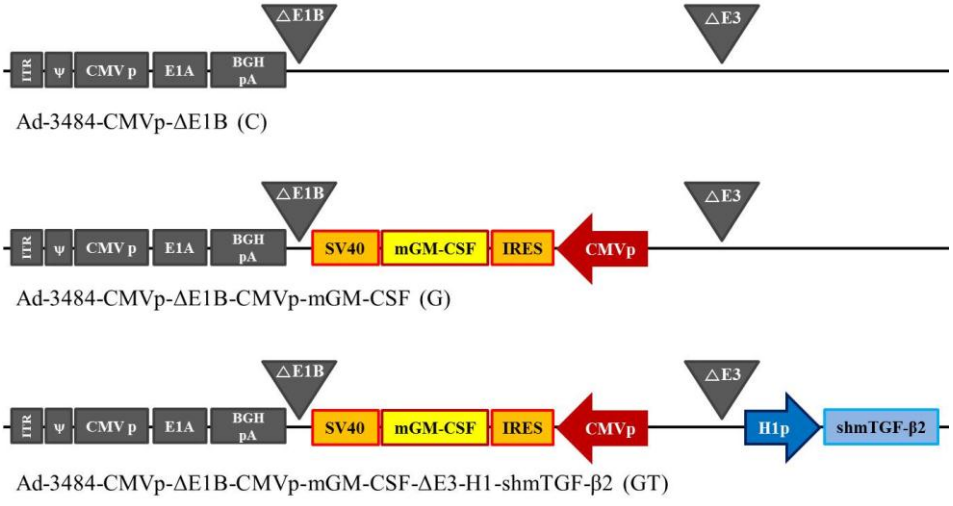
△E1B
△E3
ITR
ψ
CMV p
E1A
BGH pA
Ad-3484-CMVp-ΔE1B (C)
SV40
mGM-CSF
IRES
CMVp
Ad-3484-CMVp-ΔE1B-CMVp-mGM-CSF (G)
H1p
shmTGF-β2
Ad-3484-CMVp-ΔE1B-CMVp-mGM-CSF-ΔE3-H1-shmTGF-β2 (GT)

(B)

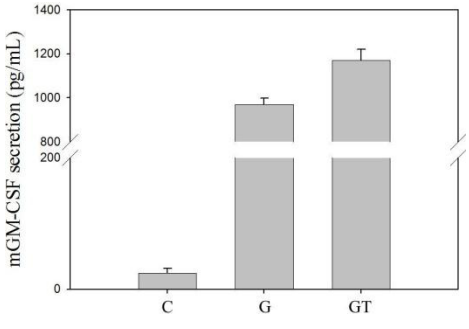
mGM-CSF secretion (pg/mL)
1400
1200
1000
800
200
0
C
G
GT

(C)

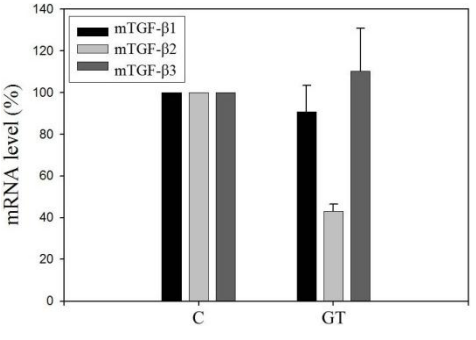
mRNA level (%)
mTGF-β1
mTGF-β2
mTGF-β3
140
120
100
80
60
40
20
0
C
GT

(D)

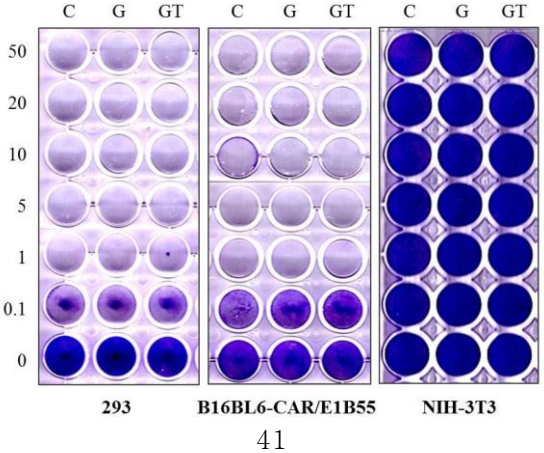
C
G
GT
50
20
10
5
1
0.1
0
293
B16BL6-CAR/E1B55
NIH-3T3

Figure 6. mGM-CSF and shmTGF-β2 expressing recombinant adenoviruses. (A) Schematic representation of adenovirus vectors expressing mGM-CSF and shmTGF-β2. Ad3484-CMVp-ΔE1B-CMVp-mGM-CSF (G) is composed of the mGM-CSF gene in the E1 region and Ad3484-CMVp-ΔE1B-CMVp -mGM-CSF-ΔE3-H1-shmTGF-β2 (GT) is composed of the shmTGF-β2 gene in the E3 region of Ad3484-CMVp-ΔE1B-CMVp-mGM-CSF. Two days after infection, mGM-CSF expression level was measured in the culture supernatants by ELISA (B) and mTGF-β mRNA was estimated by real-time-PCR (C). The oncolytic activity of these viruses was analyzed by in vitro cytopathic effect (CPE) assay. Cells were infected with each virus at an MOI of 0.1 to 50. To examine the level of mGM-CSF and mTGF-β2 mRNA expression, B16BL6-CAR/E1B55 cells were infected with virus at a MOI of 50 (D).

5. Ex vivo and in vivo testing of combination treatment with shmTGF-β2 and mGM-CSF

To demonstrate that an enhanced anti-cancer immune response was induced by recombinant adenovirus expressing both mGM-CSF and shmTGF-β2, ex vivo and in vivo tests were performed. B16BL6-CAR/E1B55 cells infected with virus at an MOI of 50 were incubated for 4 hours with splenocytes isolated from C57BL/6 mice and the cytotoxic activity was then measured with an LDH assay. Notably, the GT virus-infected cells appeared to enhance the anti-tumor activity of the splenocytes compared to the cells infected with mGM-CSF virus or shmTGF-β2 virus alone (Fig 7A).

To determine whether the same effects were induced in an animal model of melanoma, C57BL/6 mice were subcutaneously injected with B16BL6-CAR/E1B55 murine melanoma cells in the abdomen. When tumors reached 70–100 mm^3 in size, mice were intratumorally injected with PBS, the empty vector (C virus), G virus, or GT virus on days 1, 3, and 5. As shown in Figure 7B, control tumors that received PBS showed robust growth. In marked contrast, C, G, GT virus-treated tumors reached average volumes of 1719.1 ± 180.1 mm^3, 1342.5 ± 254.1 mm^3, and 810.3 ± 112.5 mm^3, respectively, by 9 days. By day 20, the C, G, or GT virus-treated tumors reached average volumes of 10746.9 ± 663.9 mm^3, 5360.6 ± 2115.0 mm^3, and 4443.8 ± 925.7 mm^3, respectively. These results indicate that the G virus can delay tumor growth

compared to the control virus and that combined treatment with mGM-CSF together with shmTGF-β2 resulted in a delayed growth rate of tumors compared with those of the mice treated with mGM-CSF alone. This enhanced anti-tumor effect for the combination treatment can be attributed to the simultaneous stimulation of a non-specific mGM-CSF-induced immune reaction and a decrease in mTGF-β2 expression. In addition, the tumor growth inhibition resulting from the decreased expression of mTGF-β2 mRNA had a positive effect on the anti-tumor response in the animal model.

(A)

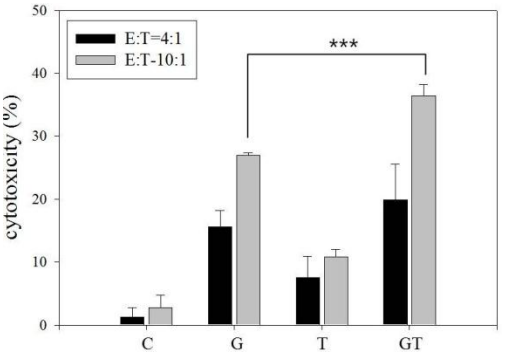

(B)

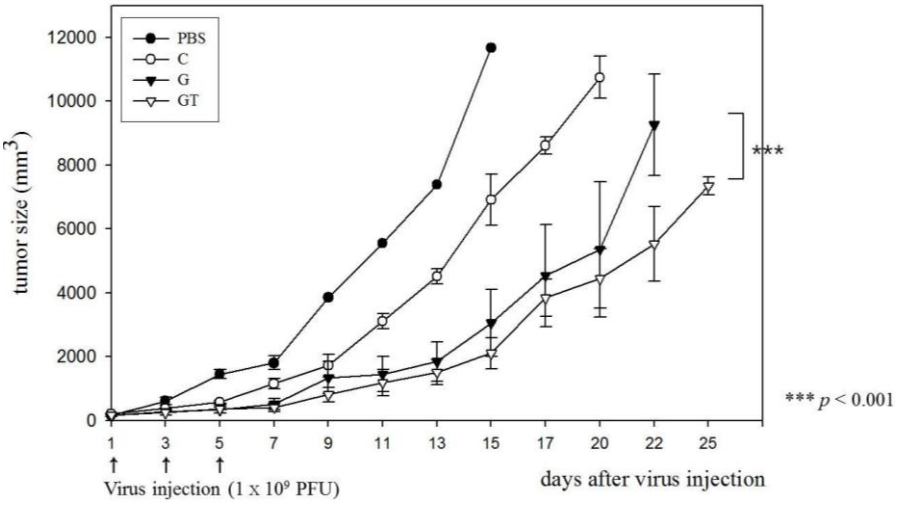

Figure 7. The anti-tumor effect of adenoviruses expressing mGM-CSF with shmTGF-β2. The anti-tumor effect of G, T, or GT virus was confirmed by ex vivo (A) and in vivo (B) experiments. (A) B16BL6-CAR/E1B55 cells infected with each virus at an MOI of 50 were incubated for 4 h with splenocytes isolated from C57BL/6 mice. The splenocyte cytotoxic activity was measured by an LDH assay. (B) C57BL/6 tumor-bearing mice were treated with

intratumoral injections of 1×10^9 PFU/50 μL of adenoviruses on days 1, 3, and 5. Tumor volume was monitored and recorded every 2 days until the end of the study. Values represent the mean ± SE (5 animals per group).

6. Construction of a recombinant adenovirus expressing MART1, mGM-CSF, and shmTGF-β2

To induce a stronger and long-term immune response, a recombinant pVAX1-MART1 plasmid and a recombinant oncolytic adenovirus expressing MART1, mGM-CSF, and shmTGF-β2 were constructed. Ad3484-CMVp-ΔE1B-MART1 (M virus) was constructed, with the objective of priming/boosting an antigen-specific immune response in the mouse melanoma cells. Ad3484-CMVp-ΔE1B-MART1-IRES-mGM-CSF-ΔE3-H1-shmTGF-β2 (MGT virus) was constructed with the aim of further enhancing the mouse melanoma antigen-specific immune response, general immune response, and suppression of cancer cell growth. MART1 and mGM-CSF, harbored in an internal ribosome entry site (IRES) expression cassette, were inserted into the E1 region of the adenovirus genome, while shmTGF-β2 was inserted into the E3 region (Fig 8A). The oncolytic activity of these recombinant adenoviruses was verified by in vitro CPE assay (Fig 8B).

(A)

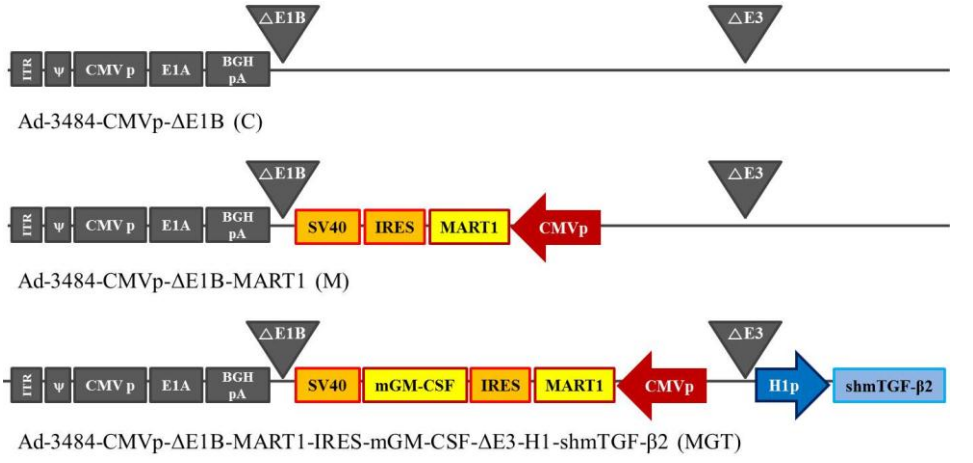

(B)

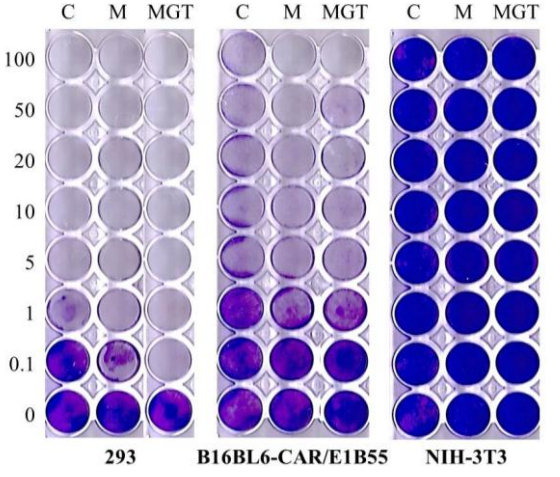

Figure 8. Schematic representation of recombinant adenovirus vectors expressing MART1/mGM-CSF/shmTGF-β2 and cytotoxic activity of viruses. (A) Ad3484-CMVp-ΔE1B-CMVp-MART1 (M) is composed of the MART1 gene in the E1 region of Ad3484-CMVp-ΔE1B. Ad3484-CMVp-ΔE1B

-MART1-IRES-mGM-CSF-ΔE3-H1-shmTGF-β2 (MGT) is composed of the MART1 and mGM-CSF genes in the E1 region and shmTGF-β2 gene in the E3 region of Ad3484-CMVp-ΔE1B. (B) The oncolytic activity of these viruses was analyzed by in vitro cytopathic effect (CPE) assay. Cells were infected with each virus at an MOI of 0.1 to 100 and then cells were stained with 0.5% crystal violet.

7. Enhanced expression of MART, mGM-CSF, and downregulation of mTGF-β2 in MGT virus-infected mouse melanoma cells

Before progressing to animal tests to further investigate the anti-tumor effects of MGT virus, the level of recombinant oncolytic adenovirus-mediated MART1, mGM-CSF, and shmTGF-β2 expression was verified. B16BL6-CAR/E1B55 cells were infected with C, M, or MGT virus with at an MOI of 50. Two days after infection, MART1 was detected by western blotting and showed a significant increase in the endogenous cellular expression of the virally transduced MART1 (Fig 9A). Furthermore, because MART1 is located on the surface of the melanoma cells, its expression was also detected by flow cytometric analysis. This analysis showed that the surface expression of MART1 was increased on both the M and MGT virus-infected cells (Fig 9B).

To quantify the expression level of mGM-CSF induced by infection with the recombinant adenovirus, B16BL6-CAR/E1B55 cells were infected with C, G, or MGT virus at an MOI of 50 and then an mGM-CSF ELISA was performed to estimate the mGM-CSF protein concentration in the cell supernatants. The G and MGT virus-infected cells showed a significant increase in the secretion of the virally transduced mGM-CSF protein (Fig 9C) compared to the C virus-infected cells.

The downregulation of mTGF-β2 transcripts in B16BL6-CAR/E1B55 cells was confirmed by real-time-PCR. As shown in Figure 9D, mTGF-β2 mRNA

levels were decreased by more than 50% in the T or MGT virus infected B16BL6-CAR/E1B55 cells compared to control virus infected cells, while the mRNA levels of mTGF-β1 and mTGF-β3 were not changed significantly in the treated cells. Notably, the secreted level of mTGF-β2 protein was also significantly decreased in T and MGT virus-infected cells compared to the C virus-infected cells (Fig 9E).

(A)

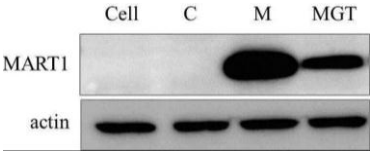

(B)

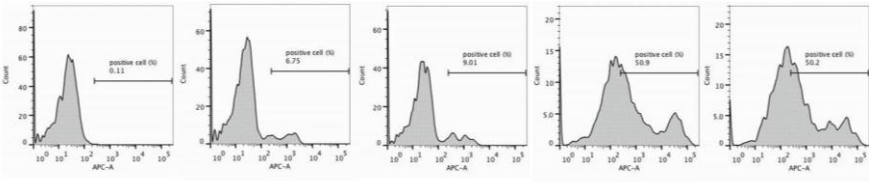

	Isotype control	Cell	C	M	MGT
Positive cell (%) :	0.11	6.75	9.01	50.09	50.2

(C)

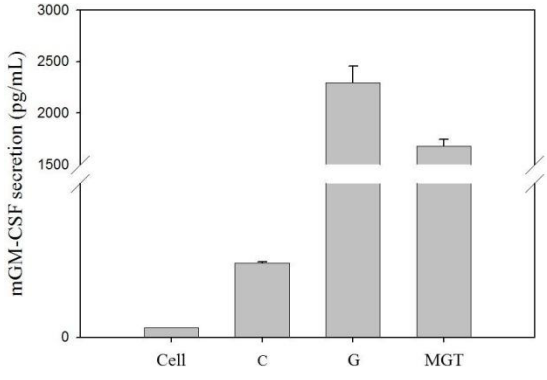

(D)

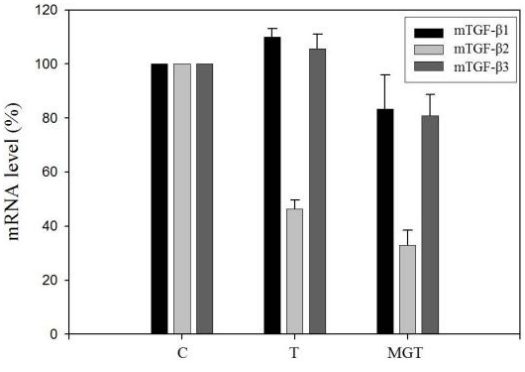

(E)

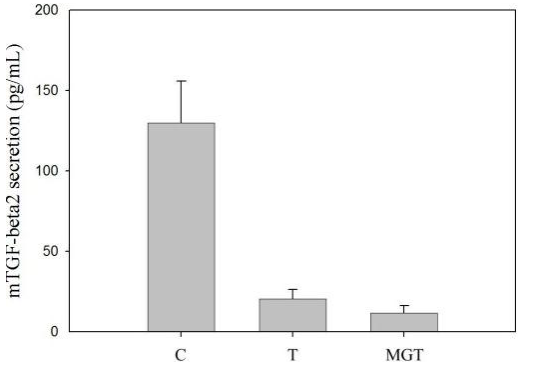

Figure 9. The expression levels of MART1, mGM-CSF, and shmTGF-β2 in virus infected cells. (A) B16BL6-CAR/E1B55 cells were infected with the C, M, or MGT virus at an MOI of 50. Two day after, MART1 endogenous expression level was detected by western blot. Actin was used as a loading control. (B) MART1 cell-surface expression level was detected by flow cytometric analysis. (C) To examine mGM-CSF level, B16BL6-CAR/E1B55 cells were infected with the C, G, or MGT virus at an MOI of 50. Two days after infection, mGM-CSF expression level was measured in the culture supernatants by ELISA. To examine mTGF-β mRNA and protein levels, B16BL6-CAR/E1B55 cells were infected with the C, T, or MGT virus at an MOI of 50. Two days after infection, mTGF-β mRNA levels were estimated by real-time-PCR (D) and mTGF-β2 protein level was measured in the culture supernatants by ELISA (E).

8. In vivo effects of combination treatment with recombinant MART1 plasmid with recombinant oncolytic adenovirus expressing MART1, mGM-CSF, and shmTGF-β2

After observing the gene expressions of recombinant adenovirus in cell culture, the next step was to evaluate the anti-tumor effects of MART1 plasmid priming together with the oncolytic adenovirus expressing MART1, mGM-CSF and shmTGF-β2 (MGT virus). To determine whether the MART1 plasmid together with the MGT virus could protect mice from tumor growth, C57BL/6 mice were subcutaneously injected with B16BL6-CAR/E1B55 mouse melanoma cells in the abdomen. Four days after the injection of tumor cells, mice were injected once intramuscularly with 50 μg of the pVAX1-MART1 plasmid. When tumors reached the size range of 70–90 mm^3, mice were intratumorally injected with PBS, C virus, M virus or MGT and the effects were monitored (Fig 10A). As shown in Figure 10B, the growth rate of tumors in mice immunized with the MART1 plasmid and the C virus was slightly delayed compared with mice treated with the MART1 plasmid and PBS. In contrast, the tumors of mice receiving both the MART1 plasmid and the MGT virus had significantly delayed growth compared to mice treated with the C virus or M virus alone, but tumor regression was not induced (Fig 10B). Images of representative virus-treated tumors can be found in Figure 11. Although mice treated with the MGT virus had delayed tumor growth and some even had

minor tumor regression, the size of the tumors still increased over time after day 23. In particular, the combination treatment of MART1 plasmid together with the M virus alone did not induce an effective anti-tumor response. It is possible that these minimal results were caused by only administering a single injection of MART1 plasmid as a booster, an amount that may not be sufficient to induce a strong mouse melanoma antigen-specific immune reaction.

To analyze the infection rate of the adenovirus vector and the infiltration of immune cells to tumor tissues following the injection of MART1 plasmid and adenovirus, histologic analysis of the tumor site was performed. Notably, many of the tumor tissues in the mice treated with MART1 plasmid and either C virus, M virus, or MGT virus were found to express adenovirus-specific protein, whereas those in the PBS-treated group did not (Fig 12). Furthermore, in the MART1 plasmid + MGT virus-treated group, many of the tumor tissues were observed to have increased lymphocytic infiltration compared with the tumor tissues of the groups treated with MART1 plasmid and C or M virus. To identify the types of immune cells that had infiltrated into the tumor tissues, tumor sections were examined by immunohistochemical analysis using anti-CD4 or anti-CD8 monoclonal antibodies. Higher frequencies of CD4+ and CD8+ T cells were observed in the tumors treated with MART1 plasmid and MGT virus compared to those treated with MART1 plasmid and C or M virus (Fig 12). However, denser immune cell infiltration was observed only at the

borders of the tumor tissues, which likely explains why these treatments did not completely protect the mice from tumor development. I believe that the single injection of MART1 plasmid was not sufficient to induce a robust immune priming effect in the mice, causing the effects of the combination to be muted in these experiments.

(A)

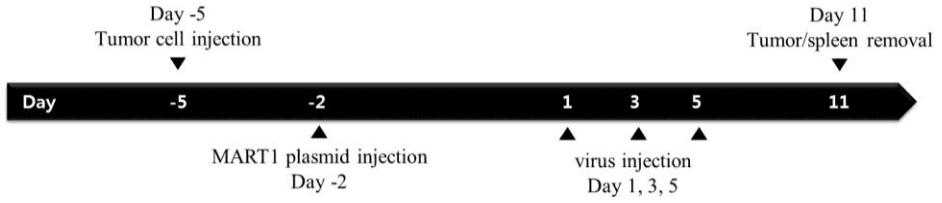

(B)

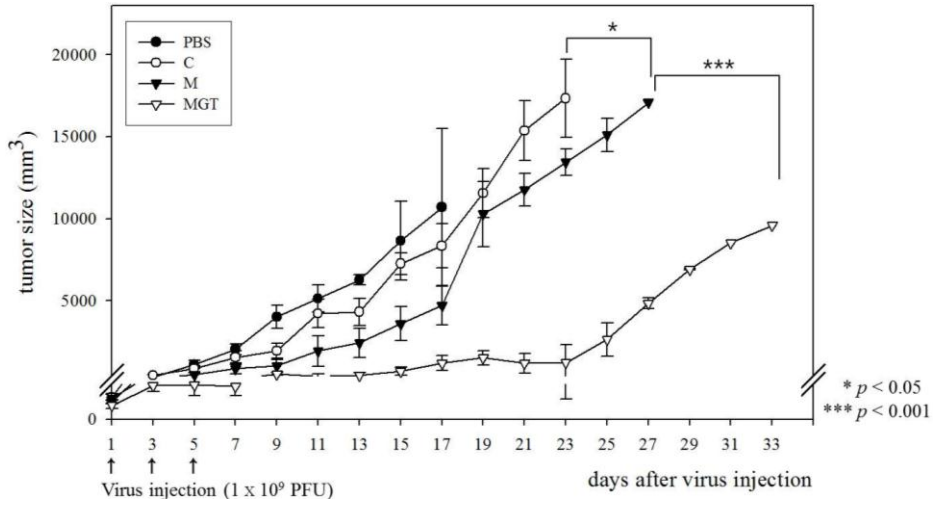

Figure 10. Anti-tumor effect of the combination treatment of MART1 plasmid with adenovirus expressing MART1, mGM-CSF, and shmTGF-β2. (A) Experimental design diagram. C57BL/6 mice were injected with 7×10^5 cells/100 μL of B16BL6-CAR/E1B55 on day -5 and treated with intramuscular injections of 50 μg/50 μL of MART1 plasmid into the rear quadriceps on day -2. C57BL/6 tumor-bearing mice were treated with intratumoral injections of 1×10^9 PFU/50 μL of adenovirus on day 1, 3, and 5. (B) Tumor volume was monitored and recorded every 2 days until the end of the study. Values represent the mean ± SE (5 animals per group).

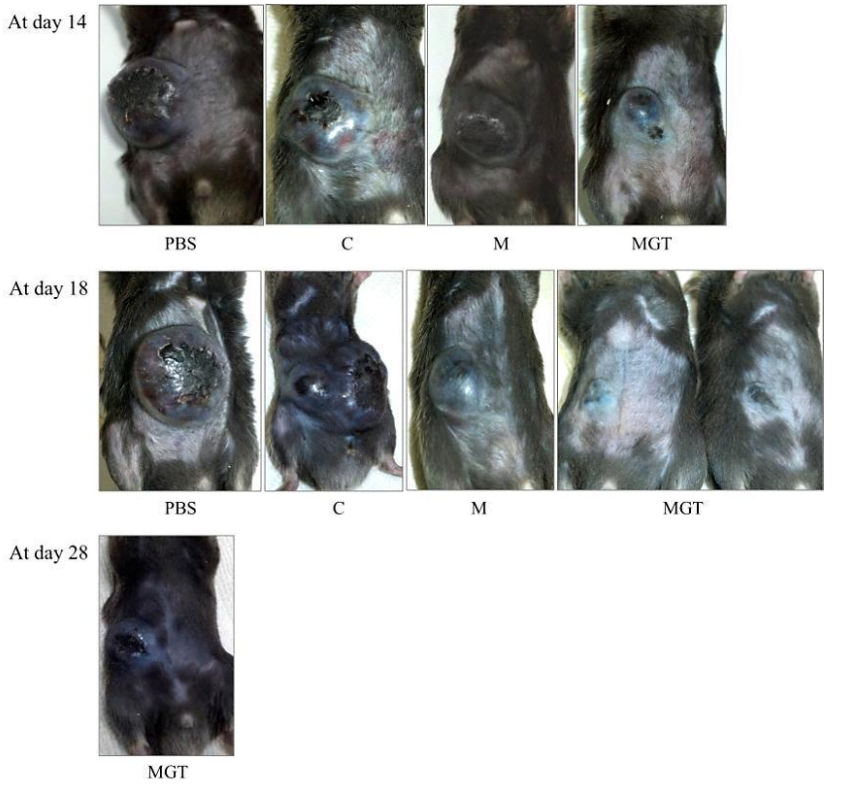

Figure 11. Tumor xenografts. Pictures of C57BL/6 tumor-bearing mice treated with virus were obtained at day 14, 18, and 28.

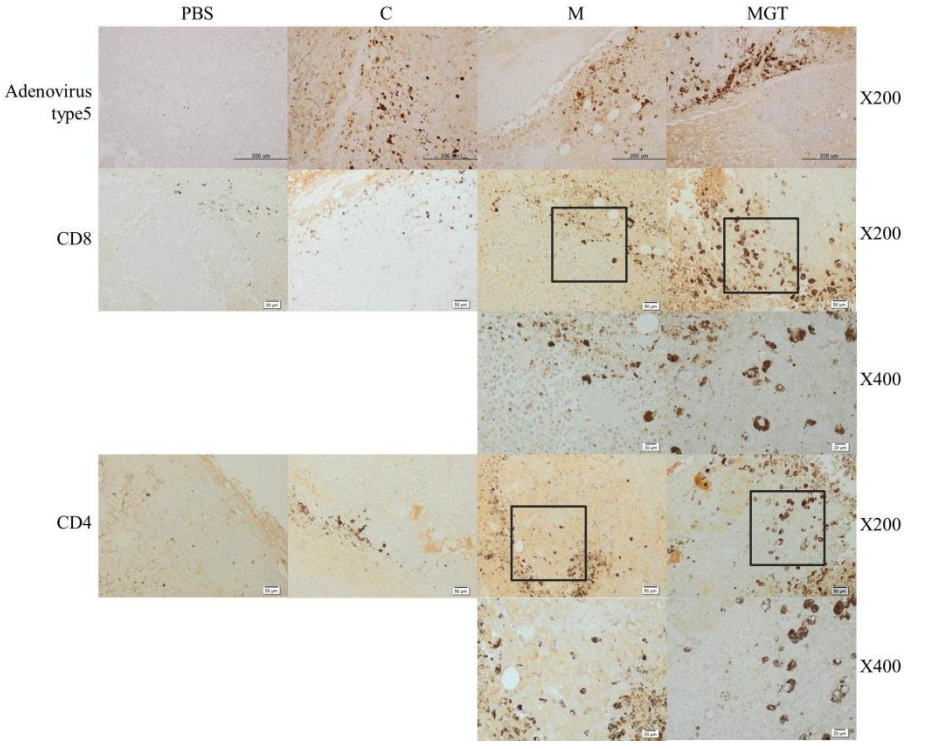

Figure 12. Immunohistochemical analysis of recombinant adenovirus infected tumor sections. C57BL/6 mice were injected with 7×10^5 cells/100 μL of B16BL6-CAR/E1B55 on day -5 and treated with intramuscular injections of 50 μg/50 μL of MART1 plasmid into the rear quadriceps on day -2. C57BL/6 tumor-bearing mice were treated with intratumoral injections of 1×10^9 PFU/50 μL of adenovirus on day 1, 3, and 5. Tumors were collected at day 11 for histological analysis. Paraffin-embedded sections of tumor tissue were stained with anti-adenovirus type 5 (top row, original magnification: ×200), anti-CD8 (second and third row, original magnification: ×200 and ×400), and anti-CD4 (fourth and fifth row, original magnification: ×200 and ×400) antibodies.

9. Immune priming/boosting effect of repeated administration of MART1 plasmid and treatment with recombinant adenovirus expressing MART1

To test the hypothesis that a single injection of MART1 plasmid did not sufficiently prime/boost the immune system enough to protect mice against melanoma, the effect of repeated injections of MART1 plasmid was investigated. The repeated administration of MART1 plasmid did in fact enhance the anti-tumor effects of the adenoviral treatment in the isolated splenocytes compared to a single injection of MART1 plasmid (Fig 13A). Furthermore, using an interferon (IFN)-γ ELISPOT assay, I determined that repeated injections of MART1 plasmid could generate a stronger mouse melanoma antigen-specific immune response via increased IFN-γ production (Fig 13B, C). Following these results, the in vivo anti-tumor effect of treatment with MART1 plasmid and the MGT virus was investigated again, with the experimental conditions changed to include repeated injections of the MART1 plasmid into mice.

(A)

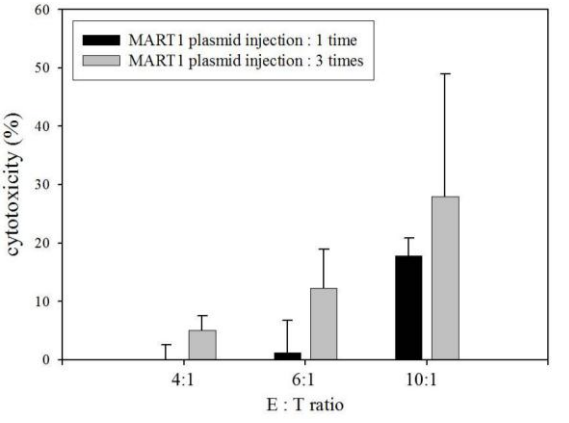

(B)

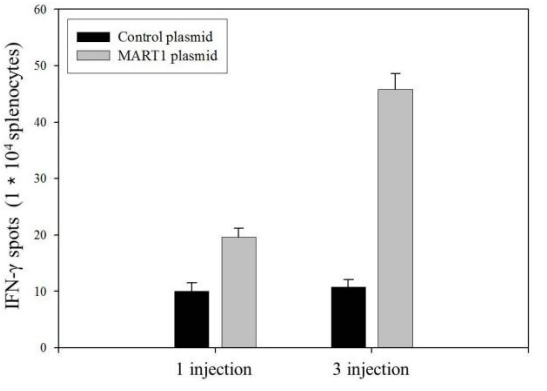

(C)

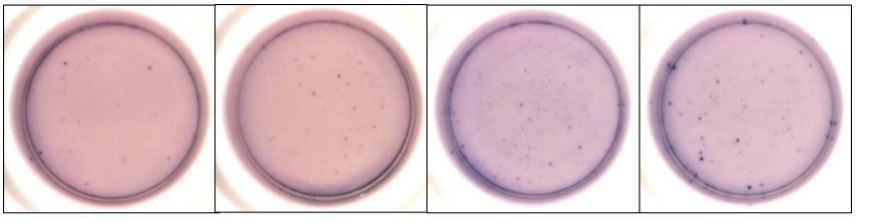

Figure 13. Effect of repeated administration of the MART1 plasmid. The

anti-tumor effect of repeated injection of MART1 plasmid was determined by ex vivo experiment. C57BL/6 mice were injected with 7×10^5 cells/100 μL of B16BL6-CAR/E1B55 on day -7 and treated with intramuscular injections of 50 μg/50 μL of MART1 plasmid into the rear quadriceps on day -14, -10, and -6 (three times injection group) or treated with intramuscular injections of 50 μg/50 μL of MART1 plasmid on day -6 (one time injection group). C57BL/6 tumor-bearing mice were treated with intratumoral injections of 1×10^9 PFU/50 μL of M virus on days 1, 3, and 5. Six days after the last virus injection, splenocytes were isolated from mice. (A) B16BL6 cells were incubated with splenocytes for 4 h and the splenocyte cytotoxic activity was then measured by LDH assay. (B) Splenocytes were stimulated with B16BL6 cell lysate for 24 h and IFN-γ ELISPOT assays were then carried out. The number of spots was counted at a concentration of 1×10^4 splenocytes. Each value represents the mean spot number ± SE of triplicates from a representative experiment. The experiment was repeated twice. (C) Representative examples of spot-forming cell response.

10. Enhanced anti-tumor effects and survival rate following repeated MART1 plasmid injections combined with MGT virus treatment

C57BL/6 mice were injected intramuscularly with 50 μg of the pVAX1-MART1 plasmid two times before tumor cell injection and one time after the injection of tumor cells into the rear quadriceps, with each injection separated from the others by a 4-day interval. When tumors reached the size range of 70–90 mm^3, mice were intratumorally injected with PBS, C virus, M virus, or MGT virus in order to compare the anti-tumor effects of MART1 plasmid and M virus with those of MART1 plasmid and MGT virus (Fig 14A). The tumor volumes by day 15 following viral treatment were 4190.9 ± 882.5 mm^3 (PBS), 627.7 ± 196.3 mm^3 (C virus), 137.7 ± 66.9 mm^3 (M virus), 384.9 ± 150.4 mm^3 (GT virus), and 0.7137 ± 0.7137 mm^3 (MGT virus). Notably, the decrease in tumor growth in the C virus-treated mice was likely caused by the tumor-cell-specific lysis induced by the oncolytic adenovirus. However, the tumor volumes of mice treated with adenovirus alone (C virus) increased over time (Fig 14B).

In the group treated with MART1 plasmid and M virus, the tumors of two mice disappeared by day 17. In contrast, the tumor volumes of the three other mice in this group increased over time after day 15 (Fig 14B, 15A), indicating that overall tumor growth was decreased compared to the PBS- and C virus-treated groups. This phenomenon is likely related to an increase in the

mouse melanoma antigen-specific immune reaction. In cell culture, the cytotoxicity of this treatment in splenocytes (isolated from mice treated with MART1 plasmid and M virus) co-cultured with B16BL6 cells was increased compared to those isolated from mice injected with MART1 plasmid with C virus. However, there was no effect of treatment with MART1 plasmid together with M virus in the LLC cell line, indicating that this human MART1 induced immune activation is in fact specific to mouse melanoma antigen (Fig 16A). In addition, a remarkably high frequency of cells producing IFN-γ was observed in mice treated with MART1 plasmid and M virus compared to mice receiving PBS, C, or GT virus (Fig 16B, C).

Interestingly, in the group treated with MART1 plasmid and MGT virus, tumor growth did not occur in four of the five mice, and the injected tumor cells of those four mice had been completely eliminated by day 15, while the tumor of the fifth mouse was gone by day 22 (Fig 14B, 15A). These data indicate that a synergistic relationship exists between the mGM-CSF, shmTGF-β2, and MART1-induced mouse melanoma antigen-specific immune response. The cytotoxic activity of splenocytes isolated from mice treated with MART1 plasmid together with MGT virus was strong and the frequency of cells producing IFN-γ was highest in the mice treated with MART1 plasmid together with MGT virus (Fig 16). Immunohistochemical analysis also showed that a higher frequency of NK cells, NK T cells, dendritic cells, and macrophages (all

of which were identified as NK1.1 or CD11b+c positive) infiltrated the tumors treated with MART1 plasmid and MGT virus compared to those treated with MART1 plasmid and C or M virus (Fig 17).

In addition, the survival rate of mice treated with MART1 plasmid and MGT virus was greatly improved, even more so than the MART1 plasmid and M virus-treated group (which was also increased), compared to mice treated with MART1 plasmid and the C virus or GT virus alone. Further, 100% of the animals that received repeated MART1 plasmid treatments and injection of MGT virus were still viable 43 days after the initial virus treatment without any recurring tumor growth (Fig 15B). Taken together, these results indicate that the combination of repeated MART1 plasmid treatment together with MGT virus injection is a very effective anti-tumor therapy for malignant melanoma.

(A)

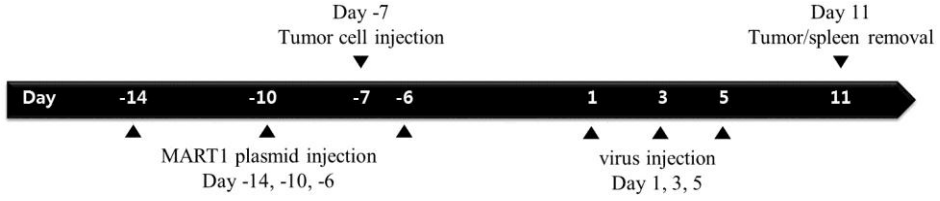

(B)

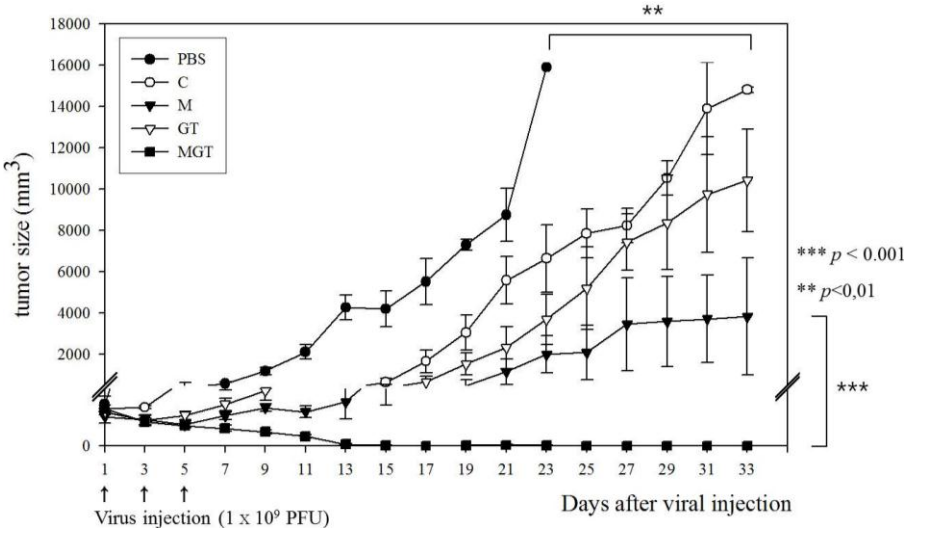

Figure 14. Anti-tumor effects induced by treatment with the recombinant MART1 plasmid and the recombinant oncolytic adenovirus expressing MART1, mGM-CSF, and shmTGF-β2. (A) Experimental design diagram. C57BL/6 mice were injected with 7×10^5 cells/100 μL of B16BL6-CAR/E1B55 on day -7 and treated with intramuscularly injections of 50 μg/50 μL of MART1 plasmid into the rear quadriceps on day -14, -10, and -6. C57BL/6 tumor-bearing mice were treated with intratumoral injections of 1×10^9 PFU/50 μL of PBS, C, M, GT, or MGT virus on day 1, 3, and 5. (B) Tumor volume was monitored and recorded every 2 days until the end of the study. Values represent the mean ± SE.

(A)

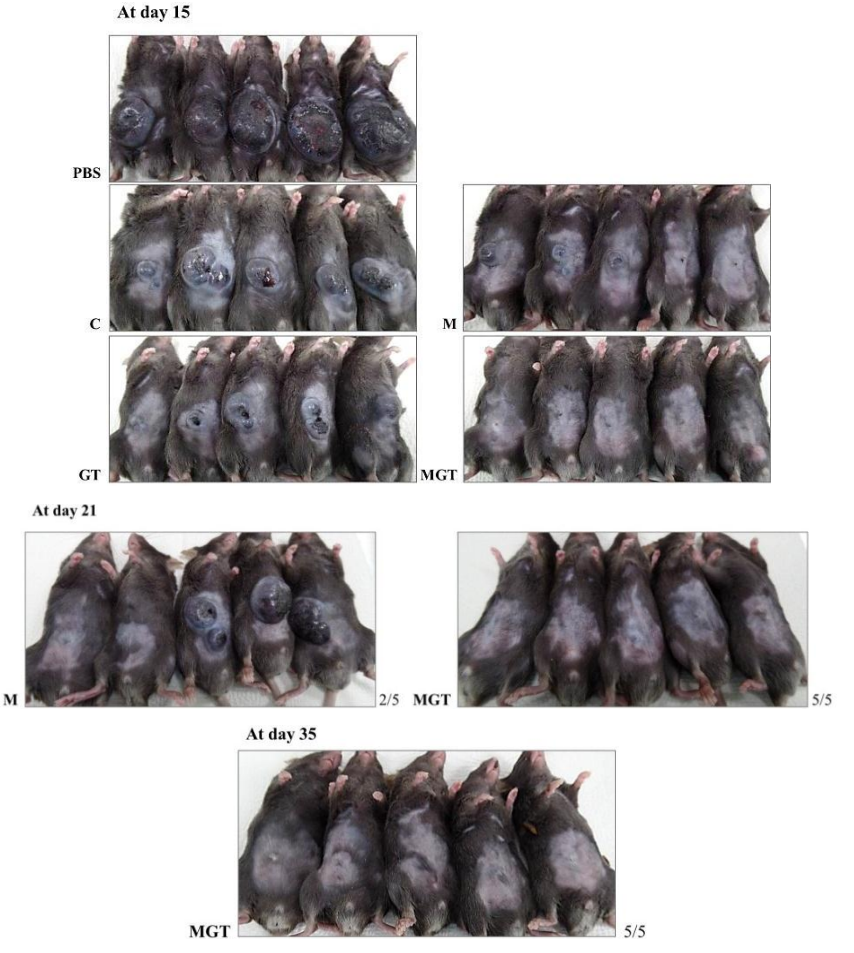
At day 15
PBS
C
M
GT
MGT
At day 21
M
2/5
MGT
5/5
At day 35
MGT
5/5

(B)

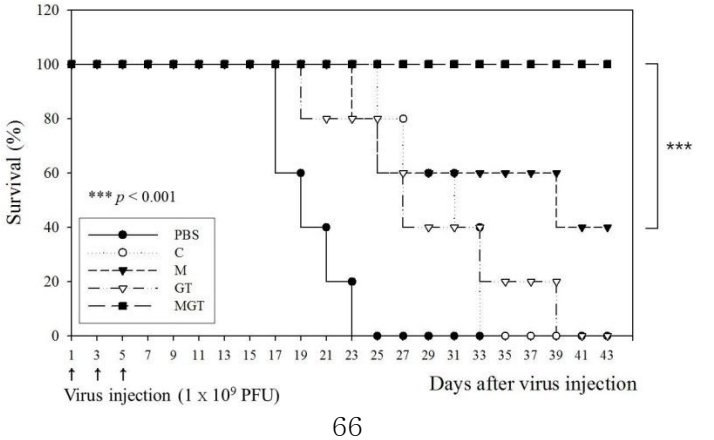
Survival (%)
120
100
80
60
40
20
0
*** p < 0.001
PBS
C
M
GT
MGT
***
1 3 5 7 9 11 13 15 17 19 21 23 25 27 29 31 33 35 37 39 41 43
Virus injection (1 x 10⁹ PFU)
Days after virus injection

Figure 15. Tumor growth and consequent survival rate of tumor-bearing mice. (A) Pictures of tumors were obtained on day 15, 21, and 35. (B) Survival rate of mice given PBS, C, M, GT, or MGT virus until day 43. One hundred percent of the animals that received MART1 plasmid and the MGT virus and 40 % of the animals that received MART1 plasmid and the M virus were still alive on day 43 without tumor occurrence and metastasis.

(A)

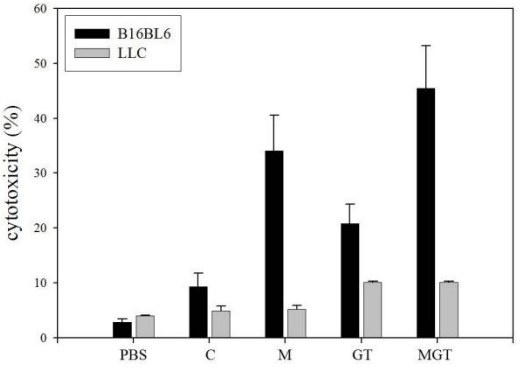

(B)

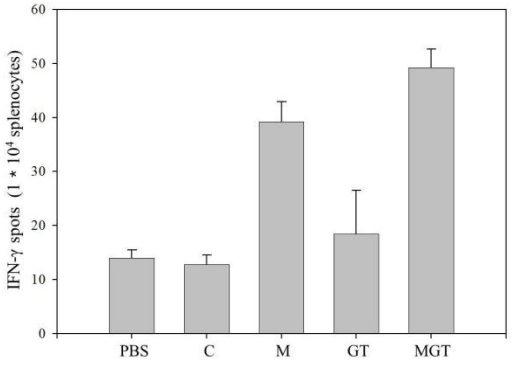

(C)

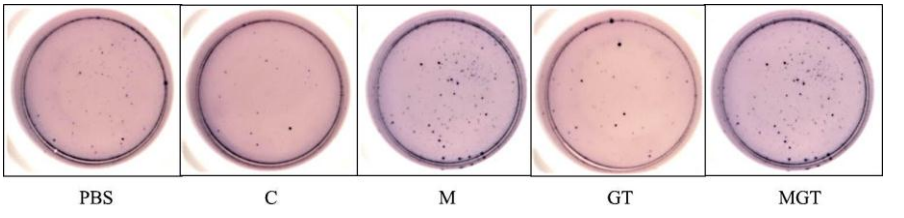

Figure 16. Enhanced mouse melanoma antigen-specific anti-tumor activity of immune cells. C57BL/6 mice were injected with 7×10^5 cells/100 μL of

B16BL6-CAR/E1B55 on day -7 and treated with intramuscular injections of 50 μg/50 μL of MART1 plasmid into the rear quadriceps on day -14, -10, and -6. C57BL/6 tumor-bearing mice were treated with intratumoral injections of 1×10^9 PFU/50 μL of PBS, C, M, GT, or MGT virus on day 1, 3, and 5. Six days after the last virus injection, the splenocytes were isolated and collected. (A) B16BL6 and LLC cells were incubated with splenocyte for 4 h and the splenocyte cytotoxic activity was then measured by using a LDH assay (Effector : Target = 10 : 1). (B) Splenocytes were stimulated with B16BL6 cell lysate for 24 h and IFN-γ ELISPOT assays were then carried out. The number of spots was counted at a concentration of 1×10^4. Each value represents the mean spot number ± SE of triplicates of a representative experiment. The experiment was repeated twice. (C) Representative examples of spot-forming cell response.

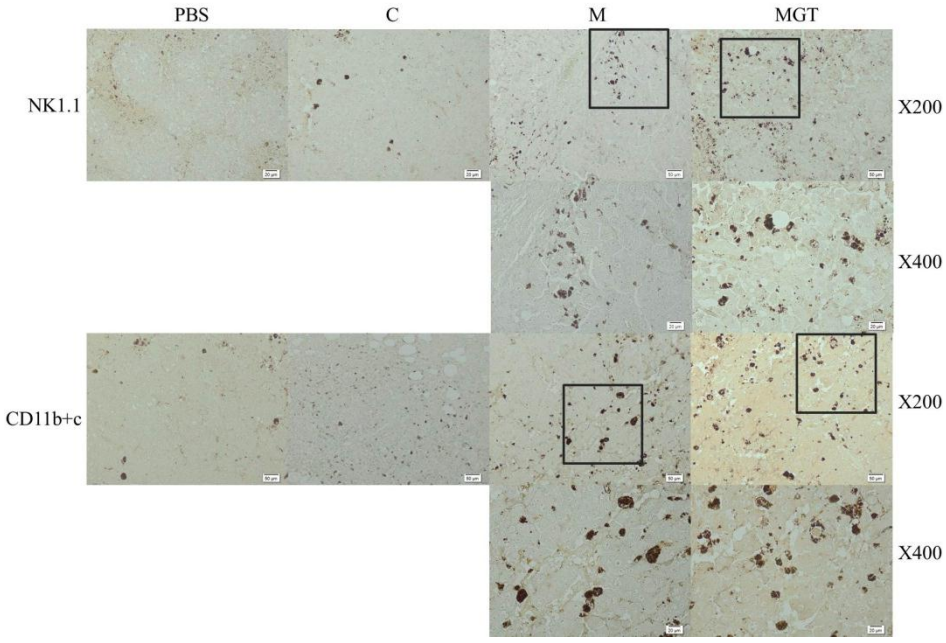

Figure 17. Detection of infiltrated immune cells by immunohistochemistry. C57BL/6 mice were injected intramuscularly with 50 μg of pVAX1-MART1. Injections were performed twice before tumor injection and once after tumor injection into the rear quadriceps, separated by a four-day interval. When tumors reached a range of 70–90 mm^3, mice were intratumorally injected with PBS, C, M, or MGT virus. Tumors were collected at day 11 for histological analysis. Paraffin-sections of tumor tissue were stained with anti-NK1.1 (top and second row, original magnification: ×200 and ×400) and anti-CD11b+c (third and fourth row, original magnification: ×200 and ×400) antibodies. NK1.1 is a key marker of NK and NKT cells. CD11b is a key marker of macrophages and CD11c is a key marker of dendritic cells.

IV. DISCUSSION

Cancer therapies, such has radiation and chemotherapy, often rely on toxic, non-specific treatments or compounds that can compromise patient health. Further, for patients with late stage cancer, such as malignant melanoma, the feasible treatment options are even more limited and often result in poor prognosis and/or relapse. In this study, I have analyzed the effectiveness of MART1 plasmid pre-treatment and injection of oncolytic adenovirus expressing MART1, GM-CSF, and shTGF-β2 to induce an anti-melanoma immune response. In doing so, I have not only highlighted the necessary protocol for immunogene treatment of this tumor type (e.g., use of adenovirus, priming/boosting the immune system with MART1 plasmid, injection site, etc.), but I have also identified a potent combination treatment (MART1, GM-CSF, and shTGF-β2 expressed in an oncolytic adenovirus) to combat tumor growth in a mouse model.

In this investigation, I have circumvented the poor adenoviral transduction efficiency in murine tumors, which is one of the major limiting factors for in vivo experiments, by using an engineered murine melanoma cell line. Poor transduction of the adenoviral vectors is likely due to the limited expression of the adenovirus type 5 receptors, the coxsackievirus and adenovirus receptor (CAR), and αvβ3 and αvβ5 integrins on the surface of mouse tumor cells. Lack

of these receptors is likely to blame for why oncolytic adenovirus has been found to only induce a low level of cell lysis in mouse tumor cells. To overcome this limitation, the B16BL6-CAR/E1B55 mouse melanoma cell line expressing CAR and E1B55 was developed, and shown to effectively replicate oncolytic adenovirus (Fig 2) [48]. This cell line, in addition to in vivo animal models, is an essential asset to the field of research investigating adenovirus-mediated treatment of melanoma. Notably, this low adenovirus infection efficiency in mouse tumor cells is not an issue in human tumor cells, which do express the necessary cell surface receptors.

Ad-3484-CMVp-ΔE1B is a replication-competent adenovirus that contains the early region 1A (E1A) gene, which is controlled by the CMV promoter, but lacks the E1B gene (Fig 4B). The tumor-specific lytic activity (oncolysis activity) of this adenovirus is modulated by the presence of the E1A gene and absence of the E1B55 gene. Further, the proteins encoded by the E1A gene of human adenovirus type 5 activate viral transcription and re-program cellular gene expression in the infected cells, thereby providing an optimal environment for viral replication [49]. E1A binding to retinoblastoma protein (Rb) is also critical for the upregulation of adenovirus E2 gene expression and transcriptional activation of cell cycle S-phase entry genes [50,51]. Therefore, the E1A gene contained in this specific adenovirus can induce active viral replication in infected cells, resulting in efficient gene transfer.

Notably, in a normal, non-malignant cell, p53 functions as an anti-viral defense by inducing growth arrest or apoptosis [52]. However, most viruses come equipped with several early gene products that prevent p53 from performing this function. For example, the E1B 55-kDa and E4 Orf6 proteins as well as several other cellular proteins can form an E3 ubiquitin ligase that targets p53 for proteasomal degradation [53-55]. The E1B 19-kDa protein is also known to block apoptosis downstream of p53 [56,57], while the E4 Orf3 protein can prevent the transcription of p53-dependent genes [58]. The engineered adenovirus construct used in this study expresses E1A, allowing viral replication to occur, but does not express E1B55 gene. Thus, this virus will only induce active viral replication in cells with inactive or mutated p53 as this is the only environment that will allow this specific adenovirus to function. Interestingly, approximately 90% of all human melanomas contain inactivated wild-type p53, but the underlying mechanisms of its inactivation are not fully understood [59].

Several studies have reported the mechanistic details of p53 inactivation in various melanoma cell lines, several of which have a mutation in the $BRAF^{V600E}$ gene as well [60]. In addition, p53 inactivation has also been achieved with a deletion in the $p16^{ink4a}$ locus and mutation of the $p14^{ARF}$ gene [59,61,62]. While the mechanism of p53 inactivation in melanoma tumor cells has not been full elucidated, the lack of functional p53 in these malignant tumor cells should, theoretically, allow the Ad-3484-CMVp-ΔE1B virus to induce active oncolysis.

However, despite the oncolytic activity of the recombinant adenovirus, only slight tumor regression was observed in mice receiving the control oncolytic adenovirus (Fig 7B, 10B, 14B). It is likely that this muted effect is a result of innate anti-viral immunity in the host. An innate anti-viral response is initiated by the infected cell while simultaneously releasing chemokines to attract neutrophils, mononuclear, and NK cells [63]. The innate immune response to adenovirus can also result in reduced spreading of the virus [64]. Thus, in order to utilize adenovirus as a cancer therapy option in these cells, it is essential to overcome this immune tolerance to the virus.

B16BL6 mouse melanoma cells, the cell type used in this study, are known to express a high level of melan-A, but when injected into mice to induce tumor formation, the host's immune tolerance to the self-antigen (melan-A) only permits a weak immune response to the B16BL6 tumors [65]. To overcome this and induce an anti-B16BL6 tumor immune response, human MART1 plasmid was administered to mice as a DNA vaccine. The results of this priming vaccination indicate that human MART1 plasmid is sufficient to generate an immune response that can protect the host against mouse melanoma (Fig 3). The basis of this cross-species protective response may rely on the nearly 70% shared amino acid sequence or the 30% non-homologous amino acid sequence [28,66]. The human MART1 sequence may also contain shared peptides that efficiently bind to the C57BL/6 MHC class I molecules (H-2b) in the muscle

cells, allowing it to stimulate an effective response against the murine melan-A expressed by the B16BL6 cells. Furthermore, to induce a stronger and longer-lived mouse melanoma antigen-specific immune response, the human MART1 plasmid and the recombinant adenovirus vector expressing MART1 were administered to tumor-bearing mice. A comparatively strong anti-tumor effect of the MART1 plasmid together with the MART1 adenovirus against B16BL6 mouse melanoma was observed in cell culture (Fig 13). However, the immune priming/boosting effect of the single MART1 plasmid injection together with MART1 recombinant virus treatment in the animal model was relatively weak (Fig 10).

The repeated administration of MART1 plasmid would have the potential to induce a prolonged, stronger antigen-specific immune response at the time of tumor development. In fact, re-exposure to MART1 by repeated injections was shown to induce an enhanced immune response and anti-tumor effect on splenocytes compared with a single injection (Fig 13). Moreover, it seems likely that the frequency and timing of the MART1 plasmid injections are important for the duration and strength of the resulting immune response, particularly because B16BL6 mouse cells grow very fast. This accelerated level of cellular growth essentially negates the anti-tumor effect of the DNA vaccine injected after tumor formation as the immune response would not be induced fast enough to catch up with the rapid tumor cell proliferation. Pre-injection of DNA

before tumor formation was, therefore, essential in order to have any substantial immune system-mediated effect on tumor growth. Notably, in order to demonstrate whether the MART1 plasmid administered post-tumor development is an effective therapeutic vaccine, an alternative animal model/tumor cell line would need to be utilized. Additional work is necessary to address this specific treatment option.

Although pre-treating mice with the MART1 plasmid and following up with a post-tumor injection of MART1 expressing adenovirus appeared to induce an anti-tumor immune response, it is likely that these effects can be supplemented with other genes to further reduce tumor size. In this study, I have focused on the addition of GM-CSF, which stimulates a non-specific immune response, and silencing of TGF-β, which inhibits tumor cell survival, growth, and immune evasion.

The adenovirus-mediated expression of mGM-CSF was used to further stimulate the immune system in response to the malignant melanoma. And I chose to focus on the combined use of GM-CSF with TGF-β silencing. TGF-β is known to inhibit Th1, macrophage, and neutrophil differentiation and development in the tumor microenvironment [42]. In addition, TGF-β suppresses the function of cytotoxic T-lymphocytes, NK cells, and dendritic cells [42]. Increased expression of each of the three TGF-β isoforms has also been observed in various cancers. For example, high levels of TGF-β1 have been

detected in the gastric mucosa of gastric cancer patients and their first-degree relatives [67]. Further, the expression levels of TGF-β1, TGF-β2, and TGF-β3 are also markedly increased in hepatocellular carcinoma (HCC) [68]. Overexpression of TGF-β2 and TGF-β3 in cholangiocarcinoma has also been shown to promote tumor cell proliferation [69], while the overexpression of TGF-β contributes significantly to the development of pancreatic cancer [70]. Notably, these reports suggest that the active isoform of TGF-β may be dependent on the type of cancer.

To this end, our laboratory has performed experiments highlighting the suppression of TGF-β1 expression in breast cancer cells as well as the anti-pancreatic cancer effects of TGF-β2 expression. In the present study, shRNA was used to suppress the expression of TGF-β1 and TGF-β2, as these are the two isoforms expressed in the majority of malignant melanomas [71,72]. Although suppressing TGF-β expression would be expected to strongly inhibit tumor growth and survival, when the expression of TGF-β1 experimentally decreased, the reduction of signaling molecules involved in cell growth, survival, and metastasis were modest (Fig 5). However, silencing TGF-β2 resulted in a much more pronounced level of reduced expression for these downstream signaling molecules. Consequently, decreasing both TGF-β1 and TGF-β2 did not appear to be necessary to cure malignant melanoma, and it is clear that TGF-β2 is the major player among the three TGF-β isoforms

expressed by B16BL6 cells.

Furthermore, when TGF-β2 was silenced in combination with GM-CSF-mediated activation of the immune system an enhanced anti-tumor response was achieved. This effect was further exacerbated when used in combination with MART1 pre-treatment and MART1-expressing adenovirus injection. When the mice were treated with MART1 plasmid and injected with an oncolytic adenovirus expressing shTGF-β2, mGM-CSF, as well as MART1, this anti-tumor response included a higher frequency of various immune cells (CD4+, CD8+ T cells, NK cells, NK T cells, dendritic cells, and macrophages) in the tumors as well as an increase in tumor cell death compared to tumors treated with MART1 plasmid and empty adenovirus or adenovirus containing only one gene. These data suggest that a potent immune reaction can be induced using multiple immune modulating genes, repeated pre-tumor boosts to the immune system, and anti-tumorigenesis genes.

V. CONCLUSION

Combination immunogene therapy, which uses the simultaneous expression of diverse immune modulating genes, appears to be more effective at treating cancer compared with single gene treatments. In this study, I have stimulated immune cells with MART1, a human melanoma antigen that can induce cross-reactivity with the mouse melan-A melanoma antigen, consequently inducing a melan-A-specific anti-tumor effect in my mouse tumor model. I have also shown that the combination of tumor antigen-specific induction with MART1 (pre- and post-tumor), general immune stimulation with GM-CSF, shTGF-β2-mediated anti-tumor effects, and oncolytic function of adenovirus was more potent than the anti-tumor effects of each treatment alone. Consequentially, I believe that this treatment combination could be used as a feasible therapeutic strategy for the malignant melanoma.

REFERENCES

1. Rigel DS, Carucci JA. Malignant melanoma: prevention, early detection, and treatment in the 21st century. CA Cancer J Clin 2000;50:215-36; quiz 37-40.
2. Siegel R, Ma J, Zou Z, Jemal A. Cancer statistics, 2014. CA Cancer J Clin 2014;64:9-29.
3. Jordan EJ, Kelly CM. Vemurafenib for the treatment of melanoma. Expert Opin Pharmacother 2012;13:2533-43.
4. Trinh VA, Hwu WJ. Ipilimumab in the treatment of melanoma. Expert Opin Biol Ther 2012;12:773-82.
5. Starz H. Ipilimumab for advanced metastatic melanoma. Expert Opin Biol Ther 2012;12:981-2.
6. Bollag G, Tsai J, Zhang J, Zhang C, Ibrahim P, Nolop K, et al. Vemurafenib: the first drug approved for BRAF-mutant cancer. Nat Rev Drug Discov 2012;11:873-86.
7. Ginn SL, Alexander IE, Edelstein ML, Abedi MR, Wixon J. Gene therapy clinical trials worldwide to 2012 - an update. J Gene Med 2013;15:65-77.
8. Imperiale MJ, Kochanek S. Adenovirus vectors: biology, design, and production. Curr Top Microbiol Immunol 2004;273:335-57.
9. McConnell MJ, Imperiale MJ. Biology of adenovirus and its use as a vector for gene therapy. Hum Gene Ther 2004;15:1022-33.
10. Glasgow JN, Everts M, Curiel DT. Transductional targeting of adenovirus vectors for gene therapy. Cancer Gene Ther 2006;13:830-44.
11. Sasada T, Noguchi M, Yamada A, Itoh K. Personalized peptide vaccination: a novel immunotherapeutic approach for advanced cancer. Hum Vaccin Immunother 2012;8:1309-13.
12. Stevceva L, Abimiku AG, Franchini G. Targeting the mucosa: genetically

engineered vaccines and mucosal immune responses. Genes Immun 2000;1:308-15.

13. Fynan EF, Webster RG, Fuller DH, Haynes JR, Santoro JC, Robinson HL. DNA vaccines: protective immunizations by parenteral, mucosal, and gene-gun inoculations. Proc Natl Acad Sci U S A 1993;90:11478-82.
14. Montgomery DL, Shiver JW, Leander KR, Perry HC, Friedman A, Martinez D, et al. Heterologous and homologous protection against influenza A by DNA vaccination: optimization of DNA vectors. DNA Cell Biol 1993;12:777-83.
15. Raz E, Carson DA, Parker SE, Parr TB, Abai AM, Aichinger G, et al. Intradermal gene immunization: the possible role of DNA uptake in the induction of cellular immunity to viruses. Proc Natl Acad Sci U S A 1994;91:9519-23.
16. Danko I, and J. A. Wolff. Direct gene transfer into muscle. Vaccine 1994;12:1499–502.
17. Wolff JA, R. W. Malone, P. Williams, W. Chong, G. Ascadi, A. Jani, and, Felgner. PL. Direct gene transfer into mouse muscle in vivo. Science 1990;247:1465–8.
18. Casares S, Inaba K, Brumeanu TD, Steinman RM, Bona CA. Antigen presentation by dendritic cells after immunization with DNA encoding a major histocompatibility complex class II-restricted viral epitope. J Exp Med 1997;186:1481-6.
19. Condon C, Watkins SC, Celluzzi CM, Thompson K, Falo LD, Jr. DNA-based immunization by in vivo transfection of dendritic cells. Nat Med 1996;2:1122-8.
20. Doe B, Selby M, Barnett S, Baenziger J, Walker CM. Induction of cytotoxic T lymphocytes by intramuscular immunization with plasmid DNA is facilitated by bone marrow-derived cells. Proc Natl Acad Sci U S

A 1996;93:8578-83.

21. Ulmer JB, Deck RR, Dewitt CM, Donnhly JI, Liu MA. Generation of MHC class I-restricted cytotoxic T lymphocytes by expression of a viral protein in muscle cells: antigen presentation by non-muscle cells. Immunology 1996;89:59-67.
22. Schoenborn JR, Wilson CB. Regulation of interferon-gamma during innate and adaptive immune responses. Adv Immunol 2007;96:41-101.
23. Davis HL, Schirmbeck R, Reimann J, Whalen RG. DNA-mediated immunization in mice induces a potent MHC class I-restricted cytotoxic T lymphocyte response to the hepatitis B envelope protein. Hum Gene Ther 1995;6:1447-56.
24. Corr M, Lee DJ, Carson DA, Tighe H. Gene vaccination with naked plasmid DNA: mechanism of CTL priming. J Exp Med 1996;184:1555-60.
25. Michel ML, Davis HL, Schleef M, Mancini M, Tiollais P, Whalen RG. DNA-mediated immunization to the hepatitis B surface antigen in mice: aspects of the humoral response mimic hepatitis B viral infection in humans. Proc Natl Acad Sci U S A 1995;92:5307-11.
26. Malmberg KJ. Effective immunotherapy against cancer: a question of overcoming immune suppression and immune escape? Cancer Immunol Immunother 2004;53:879-92.
27. Hofbauer GF, Kamarashev J, Geertsen R, Boni R, Dummer R. Melan A/MART-1 immunoreactivity in formalin-fixed paraffin-embedded primary and metastatic melanoma: frequency and distribution. Melanoma Res 1998;8:337-43.
28. Ribas A, Butterfield LH, Hu B, Dissette VB, Chen AY, Koh A, et al. Generation of T-cell immunity to a murine melanoma using MART-1-engineered dendritic cells. J Immunother 2000;23:59-66.
29. Dranoff G. GM-CSF-secreting melanoma vaccines. Oncogene

2003;22:3188-92.
30. Arellano M, Lonial S. Clinical uses of GM-CSF, a critical appraisal and update. Biologics 2008;2:13-27.
31. Dranoff G, Jaffee E, Lazenby A, Golumbek P, Levitsky H, Brose K, et al. Vaccination with irradiated tumor cells engineered to secrete murine granulocyte-macrophage colony-stimulating factor stimulates potent, specific, and long-lasting anti-tumor immunity. Proc Natl Acad Sci U S A 1993;90:3539-43.
32. Roberts AB. Molecular and cell biology of TGF-beta. Miner Electrolyte Metab 1998;24:111-9.
33. Achyut BR, Yang L. Transforming growth factor-beta in the gastrointestinal and hepatic tumor microenvironment. Gastroenterology 2011;141:1167-78.
34. Massague J. TGFbeta in Cancer. Cell 2008;134:215-30.
35. Seoane J. The TGFBeta pathway as a therapeutic target in cancer. Clin Transl Oncol 2008;10:14-9.
36. Huang SS, Huang JS. TGF-beta control of cell proliferation. J Cell Biochem 2005;96:447-62.
37. Roberts AB, Sporn MB. Physiological actions and clinical applications of transforming growth factor-beta (TGF-beta). Growth Factors 1993;8:1-9.
38. Wrzesinski SH, Wan YY, Flavell RA. Transforming growth factor-beta and the immune response: implications for anticancer therapy. Clin Cancer Res 2007;13:5262-70.
39. Mapara MY, Sykes M. Tolerance and cancer: mechanisms of tumor evasion and strategies for breaking tolerance. J Clin Oncol 2004;22:1136-51.
40. Kim SY, Kang S, Song JJ, Kim JH. The effectiveness of the oncolytic activity induced by Ad5/F35 adenoviral vector is dependent on the

cumulative cellular conditions of survival and autophagy. Int J Oncol 2013;42:1337-48.

41. Pardali K, Moustakas A. Actions of TGF-beta as tumor suppressor and pro-metastatic factor in human cancer. Biochim Biophys Acta 2007;1775:21-62.
42. Elliott RL, Blobe GC. Role of transforming growth factor Beta in human cancer. J Clin Oncol 2005;23:2078-93.
43. Kim S, Buchlis G, Fridlender ZG, Sun J, Kapoor V, Cheng G, et al. Systemic blockade of transforming growth factor-beta signaling augments the efficacy of immunogene therapy. Cancer Res 2008;68:10247-56.
44. Kaufman HL, Ruby CE, Hughes T, Slingluff CL, Jr. Current status of granulocyte-macrophage colony-stimulating factor in the immunotherapy of melanoma. J Immunother Cancer 2014;2:11.
45. Mach N, Gillessen S, Wilson SB, Sheehan C, Mihm M, Dranoff G. Differences in dendritic cells stimulated in vivo by tumors engineered to secrete granulocyte-macrophage colony-stimulating factor or Flt3-ligand. Cancer Res 2000;60:3239-46.
46. Metcalf D. Hematopoietic cytokines. Blood 2008;111:485-91.
47. Simmons SJ, Tjoa BA, Rogers M, Elgamal A, Kenny GM, Ragde H, et al. GM-CSF as a systemic adjuvant in a phase II prostate cancer vaccine trial. Prostate 1999;39:291-7.
48. Kang S, Kim JH, Kim SY, Kang D, Je S, Song JJ. Establishment of a mouse melanoma model system for the efficient infection and replication of human adenovirus type 5-based oncolytic virus. Biochem Biophys Res Commun 2014.
49. Flint J, Shenk T. Adenovirus E1A protein paradigm viral transactivator. Annu Rev Genet 1989;23:141-61.
50. Whyte P, Buchkovich KJ, Horowitz JM, Friend SH, Raybuck M, Weinberg

RA, et al. Association between an oncogene and an anti-oncogene: the adenovirus E1A proteins bind to the retinoblastoma gene product. Nature 1988;334:124-9.

51. Flint J, Shenk T. Viral transactivating proteins. Annu Rev Genet 1997;31:177-212.
52. Turpin E, Luke K, Jones J, Tumpey T, Konan K, Schultz-Cherry S. Influenza virus infection increases p53 activity: role of p53 in cell death and viral replication. J Virol 2005;79:8802-11.
53. Querido E, Marcellus RC, Lai A, Charbonneau R, Teodoro JG, Ketner G, et al. Regulation of p53 levels by the E1B 55-kilodalton protein and E4orf6 in adenovirus-infected cells. J Virol 1997;71:3788-98.
54. Steegenga WT, Riteco N, Jochemsen AG, Fallaux FJ, Bos JL. The large E1B protein together with the E4orf6 protein target p53 for active degradation in adenovirus infected cells. Oncogene 1998;16:349-57.
55. Querido E, Morrison MR, Chu-Pham-Dang H, Thirlwell SW, Boivin D, Branton PE. Identification of three functions of the adenovirus e4orf6 protein that mediate p53 degradation by the E4orf6-E1B55K complex. J Virol 2001;75:699-709.
56. Rao L, Debbas M, Sabbatini P, Hockenbery D, Korsmeyer S, White E. The adenovirus E1A proteins induce apoptosis, which is inhibited by the E1B 19-kDa and Bcl-2 proteins. Proc Natl Acad Sci U S A 1992;89:7742-6.
57. White E. Mechanisms of apoptosis regulation by viral oncogenes in infection and tumorigenesis. Cell Death Differ 2006;13:1371-7.
58. Soria C, Estermann FE, Espantman KC, O'Shea CC. Heterochromatin silencing of p53 target genes by a small viral protein. Nature 2010;466:1076-81.
59. Lu M, Breyssens H, Salter V, Zhong S, Hu Y, Baer C, et al. Restoring p53 function in human melanoma cells by inhibiting MDM2 and cyclin

B1/CDK1-phosphorylated nuclear iASPP. Cancer Cell 2013;23:618-33.
60. Pollock PM, Harper UL, Hansen KS, Yudt LM, Stark M, Robbins CM, et al. High frequency of BRAF mutations in nevi. Nat Genet 2003;33:19-20.
61. Joseph EW, Pratilas CA, Poulikakos PI, Tadi M, Wang W, Taylor BS, et al. The RAF inhibitor PLX4032 inhibits ERK signaling and tumor cell proliferation in a V600E BRAF-selective manner. Proc Natl Acad Sci U S A 2010;107:14903-8.
62. Oliner JD, Pietenpol JA, Thiagalingam S, Gyuris J, Kinzler KW, Vogelstein B. Oncoprotein MDM2 conceals the activation domain of tumour suppressor p53. Nature 1993;362:857-60.
63. Thaci B, Ulasov IV, Wainwright DA, Lesniak MS. The challenge for gene therapy: innate immune response to adenoviruses. Oncotarget 2011;2:113-21.
64. Melcher A, Parato K, Rooney CM, Bell JC. Thunder and lightning: immunotherapy and oncolytic viruses collide. Mol Ther 2011;19:1008-16.
65. Zhai Y, Yang JC, Spiess P, Nishimura MI, Overwijk WW, Roberts B, et al. Cloning and characterization of the genes encoding the murine homologues of the human melanoma antigens MART1 and gp100. J Immunother 1997;20:15-25.
66. Mockey M, Bourseau E, Chandrashekhar V, Chaudhuri A, Lafosse S, Le Cam E, et al. mRNA-based cancer vaccine: prevention of B16 melanoma progression and metastasis by systemic injection of MART1 mRNA histidylated lipopolyplexes. Cancer Gene Ther 2007;14:802-14.
67. Ebert MP, Yu J, Miehlke S, Fei G, Lendeckel U, Ridwelski K, et al. Expression of transforming growth factor beta-1 in gastric cancer and in the gastric mucosa of first-degree relatives of patients with gastric cancer. Br J Cancer 2000;82:1795-800.
68. Abou-Shady M, Baer HU, Friess H, Berberat P, Zimmermann A, Graber H,

et al. Transforming growth factor betas and their signaling receptors in human hepatocellular carcinoma. Am J Surg 1999;177:209-15.

69. Lee KT, Liu TS. Expression of transforming growth factor betas and their signaling receptors in stone-containing intrahepatic bile ducts and cholangiocarcinoma. World J Surg 2003;27:1143-8.
70. Truty MJ, Urrutia R. Basics of TGF-beta and pancreatic cancer. Pancreatology 2007;7:423-35.
71. Berking C, Takemoto R, Schaider H, Showe L, Satyamoorthy K, Robbins P, et al. Transforming growth factor-beta1 increases survival of human melanoma through stroma remodeling. Cancer Res 2001;61:8306-16.
72. Reed JA, McNutt NS, Prieto VG, Albino AP. Expression of transforming growth factor-beta 2 in malignant melanoma correlates with the depth of tumor invasion. Implications for tumor progression. Am J Pathol 1994;145:97-104.

ABSTRACT (IN KOREAN)

악성 흑색종에서 DNA백신과 면역조절 유전자들을 발현하는 종양살상 아데노바이러스의 병합치료에 의한 항 종양 효과

<지도교수 김주항>

연세대학교 대학원 의과학과

김 소 영

암에 대한 면역 치료법은 환자 몸의 면역 체계를 활성화 시킴으로써 암 세포만을 특이적으로 제거하는 치료방법이다. 하지만, 암 세포들은 여러 가지 전략을 사용하여 면역 체계를 피해가며, 면역 체계가 활성화 되었더라도 활성화된 항종양 면역 반응으로부터 도피 할 수 있는 능력 또한 갖고 있기 때문에 항암 면역 치료에 많은 한계를 드러내고 있다. 따라서 이러한 한계를 극복하는 치료제를 개발하는 것이 암 치료를 위한 과제라고 할 수 있다. 또한 환자의 세포매개면역뿐만 아니라 체액성면역을 동시에 유도하는 기능은 부작용 없이 강력한 치료 효과를 유발하기 위해 면역치료제가 갖추어야 하는

기능이다.

본 연구에서는 human MART1 유전자와 MART1을 발현하는 아데노바이러스를 이용하여 강력한 흑색종 항원 특이적인 면역반응을 유도 하고자 하였다. Human MART1과 mouse melan-A는 약 70%의 유전자 서열이 일치하기 때문에 이종간의 교차 반응성에 의해 MART1을 항원으로 인식한 면역세포들이 동물모델에서 melan-A를 인식하여 항 종양효과를 나타낼 수 있다. 이 경우 MART1에 의해서 유발된 강력한 면역반응은 자가 항원인 melan-A에 대한 면역 관용을 극복하고 다양한 면역세포로 하여금 흑색종 세포를 공격하도록 유도할 수 있다.

이와 동시에 전반적인 면역반응의 활성화를 위해 MART1을 발현하는 아데노바이러스에 대식세포, 수지상세포등 다양한 면역세포의 활성화를 유도하는 GM-CSF, 그리고 암세포의 성장과 생존기능을 억제하고, 면역회피 작용을 억제하는 TGF-β2에 대한 shRNA를 추가적으로 탑재하였다.

먼저 각 유전자를 삽입한 아데노바이러스의 항 종양효과를 확인한 결과 GM-CSF나 shTGF-β2를 각각 단독으로 탑재한 경우보다 GM-CSF와 shTGF-β2를 동시에 탑재한 경우 면역세포의 활성화를 유도하는 기능도 증가하고 종양세포의

성장을 억제하는 효과로 인해 결과적으로 항 종양 효과가 증가하는 것을 동물실험을 통해 확인하였다. 이 결과를 통해 한가지 치료용 유전자를 사용하는 것보다 여러 유전자를 함께 사용하는 것이 더 효과적임을 알 수 있었다. 그리고 MART1, GM-CSF, shTGF-β2를 모두 발현하는 종양살상 아데노바이러스와 MART1 백신 유전자의 근육 주사를 함께 처리하여 항원 특이적 면역반응의 활성화, 전반적인 면역 반응의 활성화, 종양세포의 성장 억제, 종양세포 특이적인 세포용해를 모두 유도하여 항 종양 효과를 얻고자 하였다. MART1 백신 유전자를 종양이 형성되기 전, 후에 각각 2회, 1회 근육주사로 주입한 후 MART1, GM-CSF, shTGF-β2를 모두 발현하는 종양살상 아데노바이러스를 종양에 직접 주입하였다. 그 결과 모든 생쥐에서 종양이 점점 줄어들다 바이러스 처리 후 22일 전후 시점에서 종양이 모두 없어졌으며 실험용 생쥐의 100% 생존율을 확인할 수 있었다. 이러한 효과는 다양한 in vitro, in vivo, ex vivo 실험을 통하여 MART1 백신 유전자와 MART1, GM-CSF, shTGF-β2를 모두 발현하는 종양살상 아데노바이러스를 동시에 처리 함으로서 얻어지는 항 종양 면역반응의 증가임을 확인 하였다. 다만 종양살상 아데노바이러스에 의한 종양 세포 특이적인 세포

용해기능은 바이러스에 대한 면역반응으로 인해 바이러스 주입 후 초기에만 제한적으로 나타난 것으로 생각된다. 비록 초기에만 제한적으로 그 효과가 나타났지만 연구결과 얻어진 항종양효과에 긍정적인 영향을 제공한 것으로 생각된다.

결과적으로 본 연구를 통해 다양한 면역조절 유전자를 적절히 조화시켜 사용하는 것은 항 종양 면역유전자 치료법 개발에 좋은 방법임을 확인할 수 있었다. 또한 MART1 유전자 백신, 그리고 MART1, GM-CSF, shTGF-β2를 동시에 발현하는 종양살상 아데노바이러스를 함께 사용하는 병용요법 (combination therapy)은 악성 흑색종을 치료하고 환자의 생존율을 증가시키기 위한 치료법으로 이용 될 수 있다는 가능성을 제시하였다.

핵심되는 말 : 악성흑색종, 종양항원, 유전자 백신, 면역치료, 종양살상 아데노바이러스, MART1, TGF-β, GM-CSF

PUBLICATION LIST

Kim SY, Kim JH, Song JJ. c-Cbl shRNA-expressing adenovirus sensitizes TRAIL-induced apoptosis in prostate cancer DU-145 through increases of DR4/5. Cancer Gene Ther. 2013 Feb;20(2):82-7.

Kim SY, Kang S, Song JJ, Kim JH. The effectiveness of the oncolytic activity induced by Ad5/F35 adenoviral vector is dependent on the cumulative cellular conditions of survival and autophagy. Int J Oncol. 2013 Apr;42(4):1337-48.

Kim J, **Kim SY**, Kang S, Yoon HR, Sun BK, Kang D, Kim JH, Song JJ. HSP27 modulates survival signaling networks in cells treated with curcumin and TRAIL. Cell Signal. 2012 Jul;24(7):1444-52.

Kang S, Kim JH, **Kim SY**, Kang D, Je S, Song JJ. Establishment of a mouse melanoma model system for the efficient infection and replication of human adenovirus type 5-based oncolytic virus. Biochem Biophys Res Commun. 2014 Sep 30.

Sun BK, Kim JH, Nguyen HN, Oh S, **Kim SY**, Choi S, Choi HJ, Lee YJ, Song JJ. MEKK1/MEKK4 are responsible for TRAIL-induced JNK/p38

phosphorylation. Oncol Rep. 2011 Feb;25(2):537-44.

Sun BK, Kim JH, Nguyen HN, **Kim SY**, Oh S, Lee YJ, Song JJ. TRAIL-induced caspase/p38 activation is responsible for the increased catalytic and invasive activities of Akt. Int J Oncol. 2011 Jan;38(1):249-56.

Song JJ, Szczepanski MJ, **Kim SY**, Kim JH, An JY, Kwon YT, Alcala MA Jr, Bartlett DL, Lee YJ. c-Cbl-mediated degradation of TRAIL receptors is responsible for the development of the early phase of TRAIL resistance. Cell Signal. 2010 Mar;22(3):553-63.